Chapter 7

Rapidly-varied Flow-2 —Flow Measurements

7.1 INTRODUCTION

Rapidly-varied flows (RVF), by definition, have high curvatures of flow, a consequence of which is the presence of a non-hydrostatic pressure distribution in a major part of the flow. Further, these flows are essentially local phenomena in the sense that friction plays a minor role. In this chapter a few steady, rapidly-varied flow situations are discussed in detail. Since a wide variety of RVF problems occur in practice, an exhaustive coverage of all situations is not possible in a book of this nature and hence only basic and important flow types are covered. The RVFs studied in this chapter are due to: (a) sharp-crested weirs, (b) overflow spillways, (c) broad-crested weirs, (d) end depths and (e) sluice-gates. The hydraulic jump studied in Chapter 6 is an important RVF phenomenon. In the following sections emphasis is placed on the utilization of the various RVFs for flow measurement purposes.

7.2 SHARP-CRESTED WEIR

A weir is a structure built across a channel to raise the level of water, with the water flowing over it. If the water surface, while passing over the weir, separates at the upstream end and the separated surface jumps clear off its thickness, the weir is called a *sharp-crested weir*. It is also known as a *notch* or a *thin plate weir*. Sharp-crested weirs are extensively used as a fairly precise flow-measuring device in laboratories, industries and irrigation practice. The sharp-crested weirs used in practice are usually vertical metal plates with an accurately-machined upstream edge of thickness not exceeding 2.0 mm and a bevel of angle greater than 45° on the downstream face edge. The weirs come in many geometric shapes but the rectangular and triangular ones are the most commonly used.

7.2.1 Rectangular Weir

Figure 7.1 shows the definition sketch of flow over a sharp-crested rectangular weir. The water surface of the stream curves rapidly at the upstream of the weir and plunges down in a parabolic trajectory on the downstream. This surface is known as *upper nappe*. At the weir crest, the flow separates to have a free surface which initially jumps up to a level higher than the weir crest before plunging down. This surface is known as *lower nappe*. If the weir extends to the full width of the channel, the lower nappe encloses a space having air initially at atmospheric pressure. As the flow proceeds for sometime, some of the

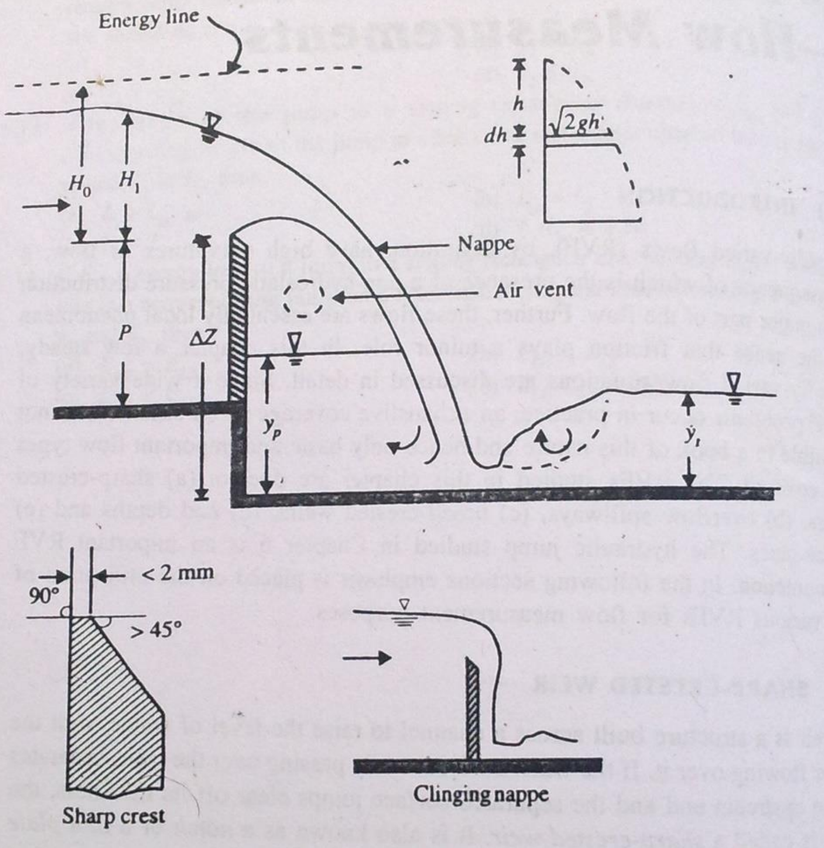

Fig. 7.1 Definition sketch of a sharp-crested weir

air from this pocket is entrained by the moving water surfaces and the pressure in the air pocket falls below the atmospheric pressure. This in turn causes the nappe surfaces to be depressed. This change is a progressive phenomenon. A limiting case of the air pocket completely evacuated is a *clinging nappe* shown in Fig. 7.1. To maintain standardised conditions for flow measurement, the air pocket below the lower nappe should be kept at a constant pressure. The atmospheric pressure in this pocket is achieved through the provision of air vents. The weir flow as above assumes at tailwater level far below the crest and is termed *free flow*. Detailed description of nappe changes and its effects on flow measurement are available in literature[1]. Figures 7.2 and 7.3 show a fully aerated and non-aerated nappe respectively.

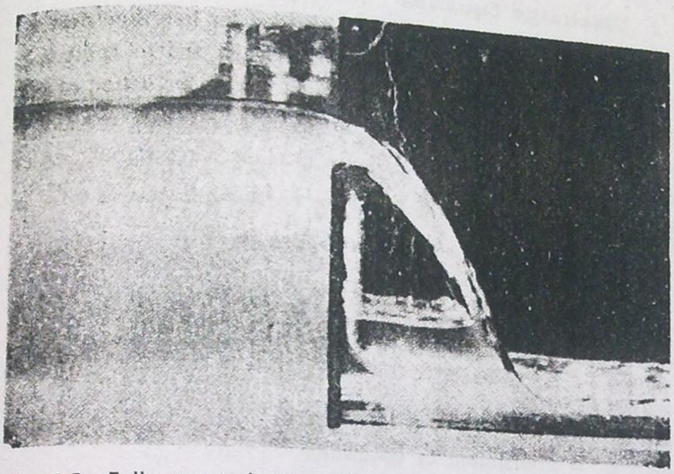

Fig. 7.2 Fully-aerated nappe (Courtesy: M.G. Bos)

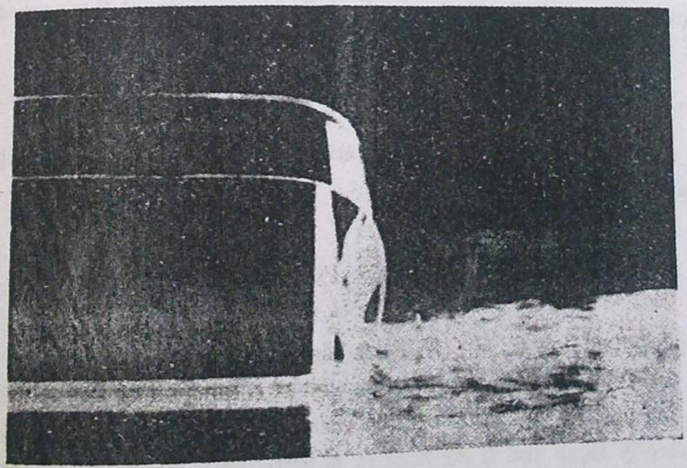

Fig. 7.3 Non-aerated nappe (Courtesy: M.G. Bos)

7.2.2 Discharge Equation

It is usual to derive the discharge equation for free flow over a sharp-crested weir by considering an ideal undeflected jet and to apply a coefficient of contraction to account for the deflection due to the action of gravity.

Thus for a rectangular weir of length L spanning the full width B of a rectangular channel (i.e. $L = B$), the ideal discharge through an elemental strip of thickness dh at a depth h below the energy line (Fig. 7.1), is given by

$$dQ_i = L\sqrt{2gh}\,dh \tag{7.1}$$

Thus the ideal discharge

$$Q_i = L\sqrt{2g}\int_{\frac{V_0^2}{2g}}^{H_1+\frac{V_0^2}{2g}} \sqrt{h}\,dh \tag{7.2}$$

and the actual discharge

$$Q = C_c\,Q_i \tag{7.3}$$

in which C_c = coefficient of contraction.

Thus

$$Q = \frac{2}{3}C_c\sqrt{2g}\,L\left[\left(H_1 + \frac{V_0^2}{2g}\right)^{3/2} - \left(\frac{V_0^2}{2g}\right)^{3/2}\right] \tag{7.4}$$

However, since Eq. (7.4) is rather inconvenient to use, the discharge equation is written in terms of H_1, the depth of flow upstream of the weir measured above the weir crest, as

$$Q = \frac{2}{3}C_d\sqrt{2g}\;LH_1^{3/2} \tag{7.5}$$

where C_d = coefficient of discharge which takes into account the velocity of approach V_0 and is given by

$$C_d = C_c\left[\left(1+\frac{V_0^2}{2gH_1}\right)^{3/2} - \left(\frac{V_0^2}{2gH_1}\right)^{3/2}\right] \tag{7.6}$$

In ideal fluid flow $C_d = f(H_1/P)$ and this variation has been studied by Stretkoff[2]. In real fluid flow C_d should in general be a function of Reynolds number and Weber number, in addition to the weir height factor H_1/P. If Reynolds number is sufficiently large and if the head H_1 is sufficiently high to make the surface tension effects negligible, the coefficient of discharge

$$C_d = f(H_1/P)$$

The variation of C_d for rectangular sharp-crested weirs is given by the well-known Rehbock formula

$$C_d = 0.611 + 0.08\frac{H_1}{P} \tag{7.7}$$

which is valid for $H_1/P \le 5.0$.

7.2.3 Sills

For very small values of P relative to H_1, i.e. for $\frac{H_1}{P} > 20$, the weir acts as a sill placed at the end of a horizontal channel and as such is termed *sill*. Assuming that the critical depth y_c occurs at the sill

$$H_1 + P = y_c = \left(\frac{Q^2}{gB^2}\right)^{1/3} \tag{7.8}$$

i.e.

$$Q = B\sqrt{g}\,(H_1 + P)^{3/2} = \frac{2}{3} C_d \sqrt{2g}\; L H_1^{3/2} \tag{7.9}$$

and

$$L = B,$$

the value of C_d from Eq. (7.9) works out to be

$$C_d = 1.06\left(1 + \frac{P}{H_1}\right)^{3/2} \tag{7.10}$$

This relationship for C_d has been verified experimentally by Kandaswamy and Rouse[3]. The variation of C_d given by Eq. (7.7) for weirs and by Eq. (7.10) for sills is shown in Fig. 7.4.

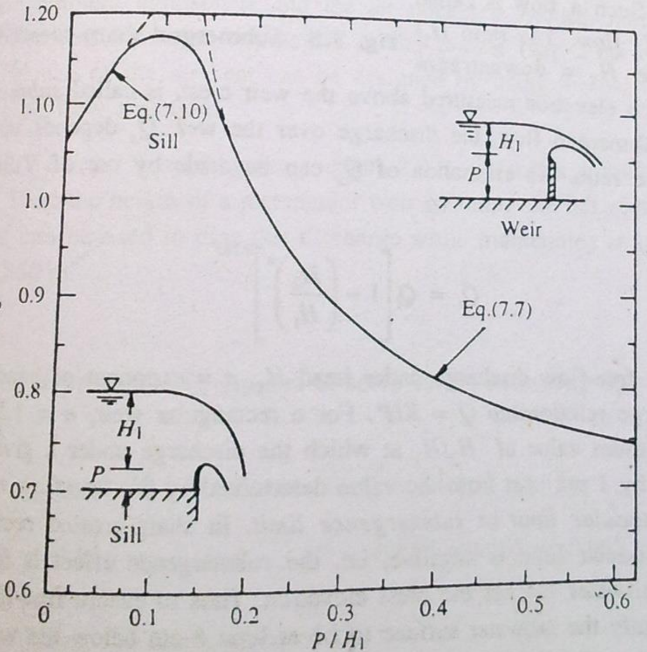

Fig. 7.4 Variation of C_d for weirs and sills

In the intermediate region of weirs and sills (i.e. $20 > H_1/P > 5$) the C_d values are expected to have a smooth transition from Eq. (7.7) to Eq. (7.10) as shown in Fig. 7.4.

A review of the effect of liquid properties on C_d is available in Ref. 1. Generally, excepting at very low heads, i.e. $H_1 \leq 2.0$ cm, for the flow of water in rectangular channels, the effects of Reynolds number and Weber number on the value of C_d are insignificant. Thus for practical purposes, Eq. (7.7) and Eq. (7.10) can be used for the estimation of discharges. The head H_1 is to be measured upstream of the weir surface at a distance of about 4.0 H_1 from the weir crest. If weirs are installed for metering purposes, the relevant standard specifications (e.g. International Standards: ISO: 1438, 1979, Thin-plate weirs) must be followed in weir settings.

7.2.4 Submergence

In free flow it was mentioned that the tailwater level is far below the crest to affect the free plunging of the nappe. If the tailwater level is above the weir crest, the flow pattern would be much different from the free-flow case (Fig. 7.5). Such a flow is called *submerged flow*. The ratio H_2/H_1, where H_2 = downstream water-surface elevation measured above the weir crest, is called *submergence ratio*. In submerged flow, the discharge over the weir Q_s depends upon the submergence ratio. An estimation of Q_s can be made by use of Villemonte formula[1,4]

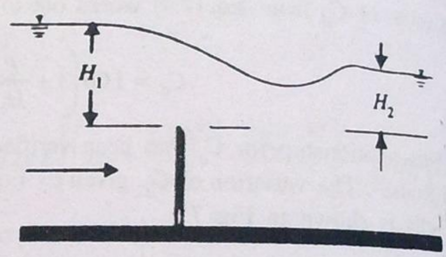

Fig. 7.5 Submerged sharp-crested weir

$$Q_s = Q_1\left[1 - \left(\frac{H_2}{H_1}\right)^n\right]^{0.385} \tag{7.11}$$

where Q_1 = free-flow discharge under head H_1, n = exponent of head in the head-discharge relationship $Q = KH^n$. For a rectangular weir, n = 1.5.

The minimum value of H_2/H_1 at which the discharge under a given head H_1 deviates by 1 per cent from the value determined by the free-flow equation is termed *modular limit* or *submergence limit*. In sharp-crested rectangular weirs the modular limit is negative, i.e. the submergence effect is felt even before the tailwater reaches the crest elevation. Thus to ensure free-flow it is usual to specify the tailwater surface to be at least 8 cm below the weir crest for small weirs. This minimum distance will have to be larger for large weirs to account for fluctuations of the water level immediately downstream of the weir due to any wave action.

available in Ref. 1.
for the flow of water
d Weber number on
poses, Eq. (7.7) and
he head H_1 is to be
out 4.0 H_1 from the
e relevant standard
, Thin-plate weirs)

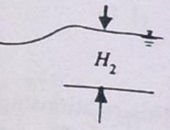

p-crested weir

ed submergence
pends upon the
of Villemonte

(7.11)

of head in the
= 1.5.
a given head
flow equation
d rectangular
is felt even
ee-flow it is
he weir crest
large weirs
tream of the

7.2.5 Aeration Need of Rectangular Weir

The need for aeration of rectangular weirs spanning the full width of a channel was indicated in Sec. 7.2.1. The rate of air supply (Q_a in m^3/s) required to completely meet the aeration need is given by[5]

$$\frac{Q_a}{Q} = \frac{0.1}{(y_p/H_1)^{3/2}} \tag{7.12}$$

in which Q = water discharge and y_p = water-pool depth on the downstream of the weir plate (Fig. 7.1). If a submerged hydraulic jump takes place, y_p can be estimated by the tailwater depth. On the other hand, for the case of a free jump occurring on the downstream, y_p can be estimated by the following empirical equation[5]

$$y_p = \Delta Z\left[\frac{Q^2}{L^2 g(\Delta Z)^3}\right]^{0.22} \tag{7.13}$$

where ΔZ = difference in elevation between the weir crest and the downstream floor (Fig. 7.1).

To cause air flow into the air pocket through an air vent, a pressure difference between the ambient atmosphere and the air pocket is needed. Assuming a maximum permissible negative pressure in the pocket (say 2 cm of water column), the size of the air vent can be designed by using the usual Darcy-Weisbach pipe flow equation.

EXAMPLE 7.1 (a) A rectangular channel 2.0 m wide has a discharge of 0.350 m^3/s. Find the height of a rectangular weir spanning the full width of the channel that can be used to pass this discharge while maintaining an upstream depth of 0.850 m.

Solution

A trial-and-error procedure is required to solve for P. Assuming C_d = 0.640, by Eq. (7.5)

$$H_1^{3/2} = 0.350\Big/\left(\frac{2}{3}\times 0.640\times\sqrt{19.62}\times 2.0\right) = 0.0926$$

$$H_1 = 0.205 \text{ m} \quad \text{and} \quad P = 0.850 - 0.205 = 0.645 \text{ m}$$

$$H_1/P = 0.318 \text{ m} \quad \text{and} \quad C_d = 0.611 + (0.08\times 0.318) = 0.636$$

2nd iteration: Using the above value of C_d

$$H_1^{3/2} = \frac{0.0926}{0.636}\times 0.640 = 0.09318$$

$$H_1 = 0.206 \text{ m},\ P = 0.644 \text{ m},\ H_1/P = 0.320$$

and

$$C_d = 0.637$$

Accepting this value of C_d, the final values are

H_1 = 0.206 m and P = 0.644 m.

The height of the required weir P = 0.644 m.

7.2.6 Contracted Weir

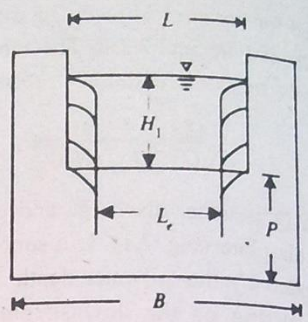

Fig. 7.6 Weir with end contractions

The discharge Eqs (7.4) and (7.5) have been derived for a weir which spans the full width of the channel. In such weirs there will be no contraction of the streamlines at the ends and as such they are termed *uncontracted* or *suppressed weirs*. However, if the length of the weir L is smaller than the width of the channel, such weirs are known as *contracted weirs* (Fig. 7.6). In contracted weirs, the flow issuing out of the weir opening will undergo contraction at the sides in addition to the contraction caused by upper and lower nappes. As a result, the effective width of the weir is reduced.

The discharge from a contracted weir can be obtained by using the effective length L_e in the Eq. (7.4). The well-known Francis formula gives

$$L_e = L - 0.1nH_1 \tag{7.14}$$

where n = number of end contractions. For the weir shown in Fig. (7.6), n = 2, and if m number of piers are introduced on a weir crest, $n = 2m + 2$. The discharge equation for the contracted weir is written as

$$Q = \frac{2}{3} C_c \sqrt{2g}\,(L - 0.1nH_1)\left[\left(H_1 + \frac{V_0^2}{2g}\right)^{3/2} - \left(\frac{V_0^2}{2g}\right)^{3/2}\right] \tag{7.15}$$

For $L > 3H_1$ and $H_1/P < 1.0$, the value of C_c is taken as $C_c = 0.622$.

For contracted sharp-crested weirs, Kindsvater and Carter[6] have given a modified version of Eq. (7.15), based on their extensive experimental investigation covering a wide range of variables, as

$$Q = \frac{2}{3} C_{dc} \sqrt{2g}\, L_e H_{1e}^{3/2} \tag{7.16}$$

where C_{dc} = coefficient of discharge for contracted weir, L_e = effective length and H_{1e} = effective head. The effective length and head are obtained as

$$L_e = L + K_L \tag{7.16a}$$

and

$$H_{1e} = H_1 + K_H \tag{7.16b}$$

where K_H and K_L are additive correction terms to account for several phenomena attributed to viscosity and surface tension. Values of recommended K_H and K_L are given in Table 7.1. The discharge coefficient C_{dc} is a function of $\frac{L}{B}$ and H_1/P, expressed as

$$C_{dc} = K_1 + K_2\left(\frac{H_1}{P}\right) \quad (7.17)$$

The variation of K_1 and K_2 are also shown in Table 7.1.

Table 7.1 Values of Parameters for Use in Eq. (7.16)*[6]

L/B	K_L (m)	K_H (m)	K_1	K_2
1.0	–0.0009	K_H = 0.001 m = Const.	0.602	+0.0750
0.9	0.0037		0.599	+0.0640
0.8	0.0043		0.597	+0.0450
0.7	0.0041		0.595	+0 0300
0.6	0.0037		0.593	+0 0180
0.5	0.0030		0.592	+0.0110
0.4	0.0027		0.591	+0.0058
0.3	0.0025		0.590	+0.0020
0.2	0.0024		0.589	–0.0018
0.1	0.0024		0.588	–0.0021

*Equation (7.16) is subject to the limitations $H_1/P < 2.0$, $H_1 > 0.03$ m, $L > 0.15$ m and $P > 0.10$ m.

EXAMPLE 7.1 (b) In Example 7.1(a) if a contracted rectangular weir of length 1.500 m and height 0.60 m is used what would be the depth of flow upstream of the weir?

Solution

In this case $\frac{L}{B} = \frac{1.50}{2.00} = 0.75$. From Table 7.1,

$$K_L = 0.0042,\ K_H = 0.001,\ K_1 = 0.596 \text{ and } K_2 = 0.0375.$$

$$L_e = L + K_L = 1.50 + 0.0042 = 1.5042 \text{ m}$$

As a trial-and-error procedure is needed to calculate H_1, assume $C_{dc} = 0.60$ for the first trial. From Eq. (7.16)

$$H_{1e}^{3/2} = 0.350 \Big/ \left(\frac{2}{3} \times 0.60 \times \sqrt{19.62} \times 1.5042\right) = 0.13133$$

$$H_{1e} = 0.2584 \text{ m},\ H_1 = 0.2584 - 0.001 = 0.2574 \text{ m}$$

$$H_1/P = \frac{0.2574}{0.60} = 0.429 \text{ and from Eq. (7.17)}$$

$$C_{dc} = 0.596 + (0.0375 \times 0.429) = 0.612$$

2nd iteration: Using the above value of C_{dc}

$$H_{1e}^{3/2} = \frac{0.13133}{0.612} \times 0.600 = 0.128755$$

$$H_{1e} = 0.255 \text{ m},\ H_1 = 0.254 \text{ m},\ H_1/P = 0.4233 \text{ and}$$

$$C_{dc} = 0.612 \text{ which is the same as the assumed value.}$$

Hence the final values are $H_1 = 0.254$ m and $C_{dc} = 0.612$. The water surface on the upstream of the weir will be at a height of 0.854 m above the bed.

7.2.7 Non-Rectangular Weirs

Sharp-crested weirs of various shapes are adopted for meeting specific requirements based on their accuracy, range and head-discharge relationships. The general form of head-discharge relationship for a weir can be expressed as $Q = KH_1^n$, where K and n are coefficients. The coefficient n depends upon the weir shape and K depends upon the weir shape and its setting. The discharge equations for some commonly used weir shapes are given in Table 7.2.

A variety of sharp-crested weir shapes have been designed to give specific head-discharge relationships and are described in literature[1]. A type of weir for which the discharge varies linearly with head, known as *Sutro Weir* finds use in flow measurement of small discharges and in automatic control of flow, sampling and dosing through float operated devices.

The details of some special sharp-crested weirs are given in the next section.

Table 7.2 Discharge Relationships for Some Commonly Used Non-Rectangular Thin Plate Weirs

Shape		*Discharge*
Triangular	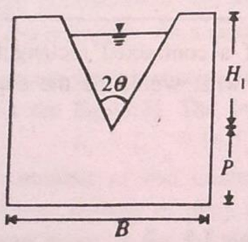	$Q=\frac{8}{15}C_d\sqrt{2g}\tan\theta\, H_1^{5/2}$ $C_d = fn(\theta)$ For $2\theta = 90°$, $C_d = 0.58$
Circular	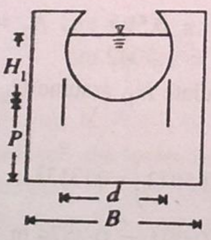	$Q = C_d\,\phi\, d^{2.5}$, $\phi = f(H_1/d)$, $C_d = f(H_1/d)$
Parabolic	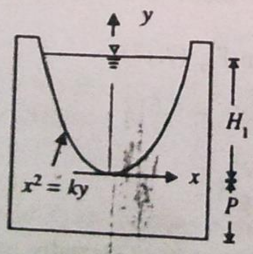	$Q=\frac{1}{4}\pi C_d\sqrt{k}\sqrt{2g}H_1^2$

Trapezoidal

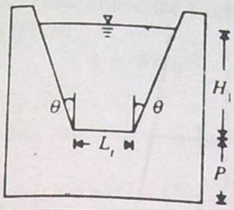

$$Q = \frac{2}{3} C_d \sqrt{2g}\, H_1^{3/2} \left(L_1 + \frac{4}{5} H_1 \tan\theta \right)$$

7.3 SPECIAL SHARP CRESTED WEIRS

7.3.1 Introduction

This section deals with special sharp-crested weirs designed to achieve a desired discharge-head relationship. These are also sometimes called *proportional* weirs (P-weirs). Since the flow over a P-weir can be controlled easily by float-regulated dosing devices, these are widely used in industry and irrigation.

Given any defined shape of weir, the discharge through it can be easily determined, e.g. in the case of a rectangular weir, the discharge is proportional to $h^{3/2}$, and in the case of a triangular weir (V-notch) the discharge is proportional to $h^{5/2}$, etc., where h is the head causing flow. The reverse problem of finding the shape of a weir to have a known head-discharge relationship constitutes the design of proportional weirs. The design of proportional weirs has considerable applications in hydraulic, sanitary and chemical engineering.

7.3.2 Linear Proportional Weir

The linear proportional weir, with its linear head-discharge characteristic is used as a control for float-regulated dosing devices, as a flow meter and as an outlet for grit chambers (sedimentation tanks). The linear proportional weir was invented by Stout (1897). This weir is only of theoretical interest as its width at base is infinite. This was improved by Sutro (1908) to develop a practical linear P-weir and is well-known as the *Sutro weir*. Referring to Fig. 7.7 the Sutro weir has a rectangular base over which a designed shape is fitted. It is found that for flows above the base weir the discharges are proportional to the heads measured above a reference plane located at one-third the depth of the base weir. Referring to Fig. 7.7.

$$Q = b\left(h + \frac{2}{3}a\right) \qquad (7.18)$$

where b = the proportionality constant.

7.3.3 Shape of the Sutro Weirs

Referring to Fig. 7.7, let the weir have the base on a rectangular weir of width $2W$ and depth a. For convenience, the horizontal and vertical axes at the origin O are chosen as y and x-axes respectively. The weir is assumed to be symmetrical about the x-axis.

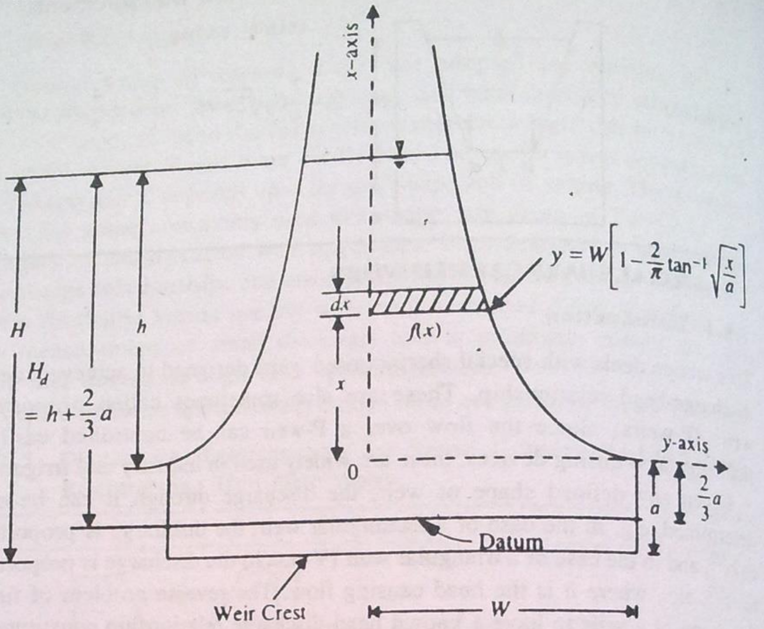

Fig. 7.7 Definition sketch of linear proportional weir

The discharge through the rectangular weir when the depth of flow is h above the origin is

$$q_1 = \frac{4}{3} W C_d \sqrt{2g}\left[(h+a)^{3/2} - h^{3/2}\right] \tag{7.19}$$

where C_d = coefficient of discharge.

The discharge through the upper portion above the origin called the *complimentary weir* is

$$q_2 = 2 C_d \sqrt{2g} \int_0^h \sqrt{h-x}\, f(x)\, dx \tag{7.19a}$$

The total discharge through the weir is

$$Q = q_1 + q_2$$

We wish this discharge to be proportional to the head measured above the reference plane situated $\frac{a}{3}$ above the crest of the weir. This reference plane is chosen arbitrarily by Sutro for mathematical convenience. Thus

$$\begin{aligned} Q &= q_1 + q_2 \\ &= \frac{4}{3} W C_d \sqrt{2g}\left[(h+a)^{3/2} - h^{3/2}\right] + 2 C_d \sqrt{2g} \int_0^h \sqrt{h-x}\, f(x)\, dx \\ &= b\left(h + \frac{2a}{3}\right) \qquad \text{for } h \ge 0 \end{aligned} \tag{7.20}$$

where b is the proportionality constant.

As there is no flow above the base weir when $h = 0$, we have by substituting $h = 0$ in Eq. (7.20)

$$b = WK\,a^{1/2}$$

where $K = 2C_d\sqrt{2g}$ (7.21)

Substituting this value of b in Eq. (7.20)

$$\frac{2}{3}W\left[(h+a)^{3/2} - h^{3/2}\right] + \int_0^h \sqrt{h-x}\; f(x)\,dx = Wa^{1/2}\left(h + \frac{2a}{3}\right) \quad (7.22)$$

Re-arranging,

$$\int_0^h \sqrt{h-x}\; f(x)\,dx = Wa^{1/2}\left(h + \frac{2a}{3}\right) - \frac{2}{3}W\left[(h+a)^{3/2} - h^{3/2}\right]$$

$$= W\left[\frac{2}{3}a^{3/2} + a^{1/2}h + \frac{2}{3}h^{3/2} - \frac{2}{3}(a+h)^{3/2}\right]$$

$$= \frac{2}{3}W\left[h^{3/2} - \frac{3}{8}a^{-1/2}h^2 + \frac{1}{16}a^{-3/2}h^3 - \frac{3}{128}a^{-5/2}h^4 + \cdots\right] \quad (7.22a)$$

It is required to find the function $f(x)$ such that Eq. (7.22a) is satisfied for all positive values of h. This is achieved by expressing $f(x)$ in a series of powers of x and determining their coefficients. A general term x^m in $f(x)$ results in a term

$$\int_0^h \sqrt{h-x}\; x^m\,dx = \int_0^h x^m\left(h^{1/2} - \frac{1}{2}h^{-1/2}x + \frac{1}{8}h^{-3/2}x^2 - \ldots\right)dx$$

$$= \text{Const}\;(h)^{m+(3/2)} \quad (7.23)$$

so that the first term in Eq. (7.22a) can be obtained by a constant term in the series for $f(x)$ and the other terms by taking m half an odd integer. Consequently we assume,

$$f(x) = y = A_1 + A_2x^{1/2} + A_3x^{3/2} + A_4x^{5/2} + \ldots \quad (7.24)$$

Substituting this in Eq. (7.22a)

$$\int_0^h \left(A_1\sqrt{h-x} + A_2\sqrt{hx - x^2} + \cdots\right)dx$$

$$= \frac{2A_1}{3}h^{3/2} + \frac{\pi A_2 h^2}{8} + \frac{\pi A_3 h^3}{16} + \frac{5\pi A_4 h^4}{128} + \cdots$$

$$= \frac{2}{3}W\left[h^{3/2} - \frac{3}{8}a^{-1/2}h^2 + \cdots\right]$$

This leads to

$$A_1 = W$$

$$A_2 = -\frac{2}{\pi}a^{-1/2}W$$

$$A_3 = \frac{2}{3\pi}a^{-3/2}W$$

and so on.

Substituting these coefficients in Eq. (7.24)

$$f(x) = W\left[1-\frac{2}{\pi}\left\{\frac{x^{1/2}}{a^{1/2}}-\frac{x^{3/2}}{a^{3/2}}+\frac{x^{5/2}}{5a^{5/2}}-\dots\right\}\right]$$

$$= W\left[1-\frac{2}{\pi}\tan^{-1}\sqrt{\frac{x}{a}}\right] \quad (7.25)$$

The discharge equation for the Sutro weir can now be summarised as

$$Q = b\left(h+\frac{2}{3}a\right) = b\left(H-\frac{a}{3}\right) = bH_d \quad (7.26)$$

where $b = WKa^{1/2}$ and $K = 2C_d\sqrt{2g}$

H = depth of flow is the channel. (It is usual practice to make the crest of the base coincide with the bed of the channel)

h = head measured from the top of the rectangular base weir

H_d = depth of water over the datum.

The sharp edged Sutro weir is found to have an average coefficient of discharge of 0.62.

A simple weir geometry, called *quadrant plate weir*, which has the linear head-discharge relationship is described in Ref. 7. This weir has the advantage of easy fabrication and installation under field conditions. Linear proportional weirs having non-rectangular base weirs are described in Ref. 8 and 9.

EXAMPLE 7.2 A Sutro weir has a rectangular base of width 30 cm and height 6 cm. The depth of water in the channel is 12 cm. Assuming the coefficient of discharge of the weir as 0.62 determine the dischage through the weir. What would be the depth of flow in the channel when the discharge is doubled? (Assume the crest of the base weir to coincide with the bed of the channel).

Solution

Given: $a = 0.06$ m, $W = 0.30/2 = 0.15$ m, $H = 0.12$ m

$$K = 2C_d\sqrt{2g} = 2\times 0.62\times\sqrt{2\times 9.81} = 5.4925$$

$$b = W\,K\,a^{1/2} = 0.15\times 5.4925\times(0.06)^{1/2} = 0.2018$$

From Eq. (7.26)

$$Q = b\left(H-\frac{a}{3}\right)$$

$$= 0.2018\left(0.12-\frac{0.06}{3}\right) = 0.02018\ \text{m}^3/\text{s}$$

$$= 20.18\ \text{litres/s}$$

When the discharge is doubled, $Q = 2\times 0.02018 = 0.04036\ \text{m}^3/\text{s}$

From Eq. (7.26), $0.04036 = 0.2018\left(H-\frac{0.06}{3}\right)$

$$\therefore H = 0.2 + 0.02 = 0.22\ \text{m}$$

$$= 22\ \text{cm}$$

7.3.4 General Equation for the Weir

Cowgill[8] and Banks[9] have shown that the curve describing the weir producing a discharge $Q = b\, h^m$ for $m \geq 1/2$ is given by

$$y = y(x) = \frac{b}{2\, C_d \sqrt{2 g \pi}} \cdot \frac{\Gamma(m+1)}{\Gamma(m - 1/2)} \cdot (x)^{(m-3/2)} \tag{7.27}$$

when $Q = \int_0^h 2\, C_d\, f(x) \sqrt{2g\,(h-x)}\; dx$

where h = head measured above the crest of the weir

x, y = coordinates along vertical and horizontal axis respectively

b = a coefficient of proportionality

C_d = coefficient of discharge of the weir

Γ = gamma function.

The relationship between the exponent m and the profile of the weir is shown in Fig. 7.8.

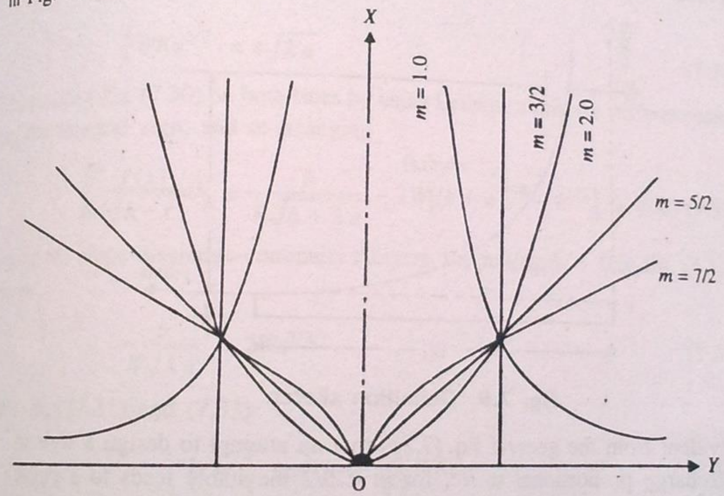

Fig. 7.8 **Weir profiles for different values of exponent** m

It is clear from Eq. (7.25) that an attempt to design a weir producing a discharge proportional to h^m for $m < 3/2$ inevitably leads to a curve which will be asymptotic at the base giving rise to infinite width, which is physically unrealizable. The linear proportional weir (m = 1) is one such case. Sutro overcame this defect by the ingeneous method of providing a rectangular base. A rational explanation for the selection of the datum was provided by Keshava Murthy[9,12,13] which is enunciated in the theorem of slope discharge continuity.

The slope-discharge-continuity theorem states: "In any physically realizable weir having a finite number of finite discontinuities in its geometry, the rate of change of discharge is continuous at all points of discontinuity." Physically this means that the curve describing the discharge versus the head for any compound weir cannot have more than one slope at any point. This is clear as otherwise it would mean, theoretically, there could be more than one value for the discharge in the infinitesimal strip in the neighbourhood of the discontinuity which is physically meaningless. The proof of this theorem which is based on the use of the theorem of Laplace transforms is beyond the scope of this book.

The P-weir consists of a known base over which a designed complimentary weir is fixed. Each weir is associated with a reference plane or datum which is determined by evaluating a new parameter λ called the *datum constant* by the application of slope discharge-continuity theorem. The problem of design of P-weirs is solved by the technique of solution of integral equations. This is explained by the design of *quadratic weirs* in the following section.

7.3.5 Quadratic Weir-notch Orifice

A quadratic weir is a proportional weir in which the discharge Q is proportional to the square root of the head h. This weir has applications in bypass flow measurement.

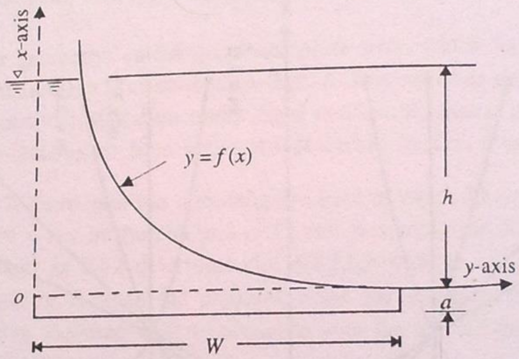

Fig. 7.9 Definition sketch

It is evident from the general Eq. (7.27) that an attempt to design a weir to pass a discharge proportional to h^m, for $m < 3/2$ inevitably leads to a curve having infinite width at the bottom which is physically unrealizable. In order to obviate this the quadratic weir is provided with a base in the form of a rectangular weir of width $2W$ and depth a, over which a designed curve is fitted (Fig. 7.9).

Referring to Fig. 7.9 the weir is assumed to be sharp-edged and symmetrical over the x-axis. When the flow is h above the base, the discharge through the rectangular weir, below the y-axis, is

$$q_1 = \frac{2}{3} WK\left[(h+a)^{3/2} - h^{3/2}\right] \quad (7.28)$$

where $K = 2C_d\sqrt{2g}$, C_d = the coefficient of discharge. The discharge from the complementary weir above the origin is

$$q_2 = K\int_0^h \sqrt{h-x}\, f(x)\, dx \quad (7.28a)$$

Total discharge $Q = q_1 + q_2 =$

$$\frac{2}{3}WK\left[(h+a)^{3/2} - h^{3/2}\right] + K\int_0^h \sqrt{h-x}\, f(x)\,dx \tag{7.29}$$

We wish to have the discharge $Q = b\sqrt{h+\lambda a}$, where b is the proportionality constant and λ is the datum constant. In other words, the discharge is proportional to the square root of the head measured above a reference plane. The constants b and λ are to be evaluated. They are determined by the two conditions of continuity of discharge and the requirement of the slope discharge continuity theorem. Rewriting Eq. (7.29)

$$Q = \frac{2}{3}WK\left[(h+a)^{3/2} - h^{3/2}\right] + K\int_0^h \sqrt{h-x}\, f(x)\,dx$$

$$= b\sqrt{h+\lambda a} \qquad \text{for } h \ge 0 \tag{7.30}$$

When $h = 0$, there is no flow above the base weir. Hence, substituting $h = 0$ in Eq. (7.30)

$$\frac{2}{3}WKa^{3/2} = b\sqrt{\lambda a} \tag{7.31}$$

Differentiating Eq. (7.30) on both sides by using Leibnitz's rule for differentiating under the integral sign, and re-arranging

$$\int_0^h \frac{f(x)}{\sqrt{h-x}}\,dh = \frac{b}{K\sqrt{h+\lambda a}} - 2W\left[(h+a)^{1/2} - h^{1/2}\right] = \phi(h) \tag{7.32}$$

Applying the slope-discharge-continuity theorem, i.e. putting $h = 0$ in Eq. (7.32), we have

$$\frac{b}{K\sqrt{\lambda a}} = 2Wa^{1/2} \tag{7.33}$$

Solving Eqs (7.31) and (7.33)

$$\lambda = \frac{1}{3} \text{ and } b = \frac{2}{\sqrt{3}}WKa \tag{7.34}$$

The reference plane for this weir is situated at $\frac{2a}{3}$ above the crest of the weir. Equation (7.32) is in the Abel's form of integral equation whose solution is[9]:

$$y = f(x) = \frac{1}{\pi}\int_0^x \frac{\phi'(h)}{\sqrt{x-h}}\,dh$$

Substituting for $\phi'(h)$

$$= W\left[1 - \frac{2}{\pi}\tan^{-1}\sqrt{\frac{x}{a}} - \frac{6}{\pi}\frac{\sqrt{x/a}}{\left(1+\frac{3x}{a}\right)}\right] \tag{7.35}$$

The weir profile drawn to scale is shown in Fig. 7.10.

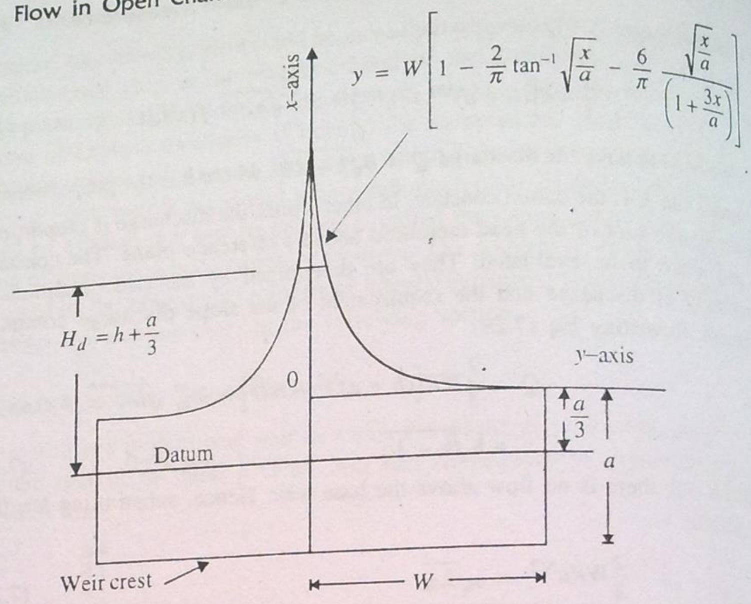

Fig. 7.10 Quadratic weir

as an orifice for all practical purposes. As this weir gives discharges proportional to the square root of the head (measured above the reference plane), both while acting as a notch as well as an orifice, this device is also called a *notch-orifice.*

The discharge equation for the quadratic weir can now be written as

$$Q = b\sqrt{h + \frac{a}{3}} = b\sqrt{\left(H - \frac{2}{3}a\right)} = b\sqrt{H_d} \qquad (7.36)$$

where $b = \frac{2}{\sqrt{3}} WKa$ and $K = 2C_d\sqrt{2g}$

and h = depth of flow above the rectangular base

H_d = head above the reference plane

H = depth of flow

Quadratic weirs having non-rectangular lower portions (base weirs) are described in detail in Ref. 14.

The quadratic weir has an average coefficient of discharge of 0.62. In a quadratic weir the error involved in the discharge calculation for a unit per cent error in head is only 0.5 per cent as against 1.5% in a rectangular weir and 2.5% in a V-notch. Hence this is more sensitive than the rectangular weir and V-notch.

EXAMPLE 7.3 A quadratic weir is designed for installation in a rectangular channel of width 30 cm. The rectangular base of the weir occupies the full width of the channel and is 6 cm in height. The crest of the base weir coincides with the channel bed. (a) Determine the discharge through the weir when the depth of flow in the channel is 15 cm. (b) What would be the depth of flow upstream of the weir when the discharge in the channel is 25 litres/s? [Assume C_d = 0.62].

Solution

Given: $a = 0.06$ m, $W = 0.30/2 = 0.15$ m, $H = 0.15$ m

$$K = 2\,C_d\sqrt{2g} = 2 \times 0.62 \times \sqrt{2 \times 9.81} = 5.4925$$

$$b = \frac{2}{\sqrt{3}}\,W\,K\,a = \frac{2}{\sqrt{3}} \times 0.15 \times 5.4925 \times 0.06 = 0.05708$$

From Eq. (7.36), $Q = b\sqrt{\left(H - \frac{2a}{3}\right)}$

(a) $Q = 0.05708 \times \left[0.15 - \left(\frac{2 \times 0.06}{3}\right)\right]^{1/2}$

$= 0.0189\ \text{m}^3\text{/s} = 18.93$ litres/s

(b) When the discharge Q = 25 litres/s = 0.025 m^3/s

From Eq. (7.36),

$$0.025 = 0.05708 \times \left[H - \left(\frac{2 \times 0.06}{3}\right)\right]^{1/2}$$

$$H = 0.1918 + 0.04 = 0.2318\ \text{m}$$

$$= 23.18\ \text{cm}$$

7.3.7 Modelling of Flow Velocity Using Special Weirs

In many hydraulic engineering situations it is desirable to maintain a constant average velocity in a channel for a range of flows. A typical example of this situation is the grit chamber used in sewage treatment. To obtain such a control of the velocity of flow in the channel, proportional weirs can be used at the outlet of the channel. The channel cross-section shape, however, will have to be determined. This, in turn, depends upon the shape of the outlet weir and the relationship between the upstream head and velocity. Design of such channel shapes controlled by a weir at the outlet is described in Refs 8 and 15. It is interesting to note that a linear proportional weir, such as a Sutro weir, fixed at the end of a rectangular channel irrespective of the fluctuations of the discharge.

7.4 OGEE SPILLWAY

The ogee spillway, also known as the *overflow spillway*, is a control weir having an ogee (S-shaped) overflow profile. It is probably the most extensively used spillway to safely pass the flood flow out of a reservoir.

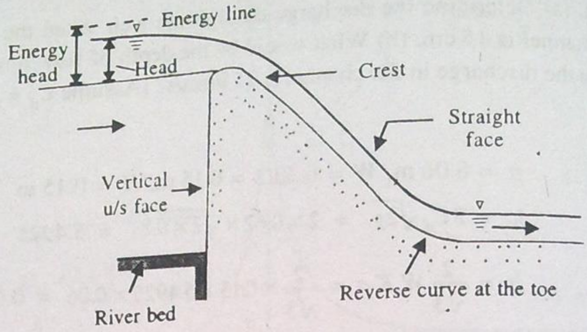

Fig. 7.11 Typical ogee spillway

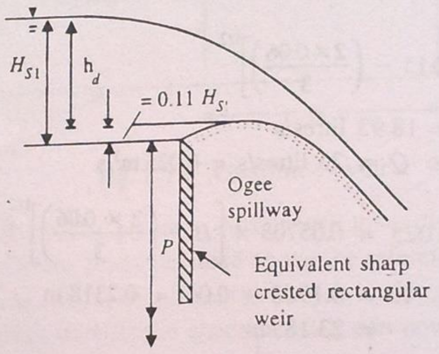

Fig. 7.12 Lower nappe as a spillway profile

A typical ogee spillway is shown in Fig. 7.11. The crest profile of the spillway is so chosen as to provide a high discharge coefficient without causing dangerous cavitation conditions and vibrations. The profile is usually made to conform to the lower nappe emanating from a well-ventilated sharp-crested rectangular weir (Fig. 7.12). This idea is believed to have been proposed by Muller in 1908. Such a profile assures, for the design head, a high discharge coefficient, and at the same time, atmospheric pressure on the weir. However, heads smaller than the design head cause smaller trajectories and hence result in positive pressures and lower discharge coefficients. Similarly, for heads higher than the design head, the lower nappe trajectory tends to pull away from the spillway surface and hence negative pressure and higher discharge coefficients result.

For a high spillway ($H_{s1}/P \simeq 0$), it is found experimentally that the spillway apex is about 0.11 H_{s1} above the equivalent sharp-crested weir crest (Fig. 7.12). The design head for the spillway is then $h_d = 0.89\ H_{s1}$. Considering the discharge equation with suffix 's' for an equivalent sharp-crested weir

$$q = \frac{2}{3}\ C_{ds}\sqrt{2g}\ H_{s1}^{3/2} \qquad \text{(for the sharp-crested weir)}$$

and $$q = \frac{2}{3} C_{d1} \sqrt{2g}\, h_d^{3/2}$$ (for the overflow spillway)

it is easy to see that $C_{d1} = 1.19\, C_{ds}$, i.e. the ogee spillway discharge coefficients are numerically about 20 per cent higher than the corresponding sharp-crested weir coefficients.

7.4.1 Uncontrolled Ogee Crest

If there are no crest gates over them, such spillways are designated as uncontrolled spillways. The crest shapes of uncontrolled ogee spillways have been extensively studied by the US Bureau of Reclamation, and accurate data relating to the nappe profiles, coefficient of discharge and other information pertinent to spillway design are available[16]. Considering a typical overflow spillway crest (Fig. 7.13) the profile of the crest downstream of the apex can be expressed as[16]

$$\frac{y}{H_d} = K\left(\frac{x}{H_d}\right)^n \tag{7.37}$$

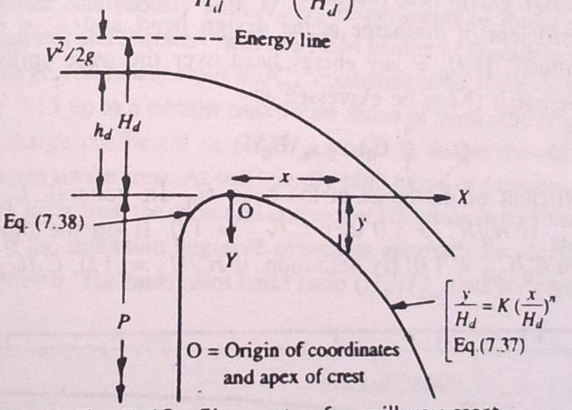

Fig. 7.13 Elements of a spillway crest

in which x and y are the coordinates of the downstream curve of the spillway with the origin of coordinates being located on the apex, H_d = design energy head, i.e. design head measured above the crest to the energy line. K and n are constants and their values depend upon the inclination of the upstream face and on the velocity of approach. For low velocities of approach, typical values of K and n are

Upstream face	K	n
Vertical	0.500	1.850
1 Horizontal : 1/3 vertical	0.517	1.836
1 Horizontal : 1 vertical	0.534	1.776

The crest profile upstream of the apex is usually given by a series of compound curves.

Cassidy[17] reported the equation for the upstream portion of a vertical faced spillway as

$$\frac{y}{H_d} = 0.724\left(\frac{x}{H_d} + 0.270\right)^{1.85} - 0.432\left(\frac{x}{H_d} + 0.270\right)^{0.625} + 0.126 \quad (7.38)$$

This is valid for the region $0 \geq \frac{x}{H_d} \geq -0.270$ and $0 \leq \frac{y}{H_d} \leq 0.126$. The same co-ordinate system as for the downstream profile [Eq. (7.37)] is used for Eq. (7.38) also.

Since the hydraulic characteristics of the approach channel vary from one spillway to another, it is found desirable to allow explicitly for the effect of the velocity of approach in various estimations related to the overflow spillway. With this in view, the expression for the design discharge Q_d over an ogee spillway at the design head is written as

$$Q_d = \frac{2}{3} C_{d0}\sqrt{2g}\, L_e H_d^{3/2} \quad (7.39)$$

in which H_d = design-energy head (i.e. head inclusive of the velocity of approach head), C_{d0} = coefficient of discharge at the design head and L_e = effective length of the spillway. If H_0 = any energy head over the ogee spillway, the corresponding discharge Q can be expressed as

$$Q = \frac{2}{3} C_0\sqrt{2g}\, L_e H_0^{3/2} \quad (7.40)$$

where C_0 = coefficient of discharge at the head H_0. In general, C_0 will be different from C_{d0}. If $H_0/H_d > 1.0$ then $C_0/C_{d0} > 1.0$. If on the other hand, $H_0/H_d < 1.0$, then $C_0/C_{d0} < 1.0$. By definition, if $H_0/H_d = 1.0$, $C_0/C_{d0} = 1.0$.

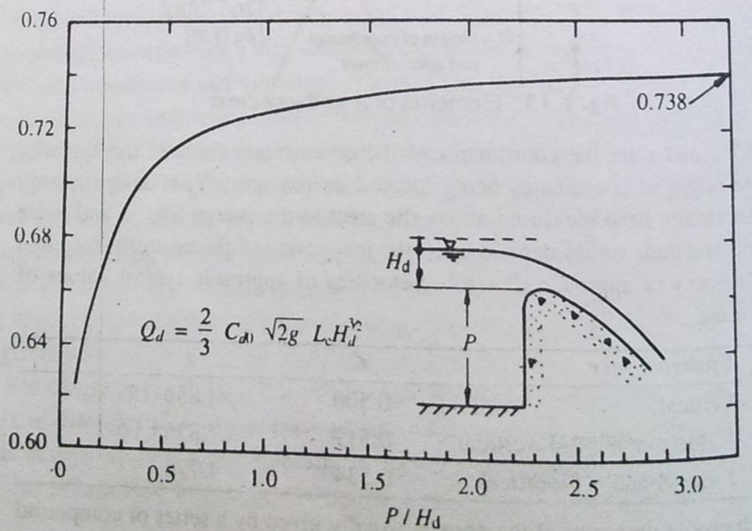

Fig. 7.14 Variation of C_{d0} with P/H_d

The discharge coefficients C_0 and C_{d0} are both functions of P/H_0 and P/H_d respectively, and of the slope of the upstream face. For a vertical faced ogee spillway, the variation of C_{d0} with P/H_d is shown in Fig. 7.14 (Ref. 18). It is seen that for $P/H_d > 2.0$, i.e. for high overflow spillways, the coefficient C_{d0} is essentially constant at a value of 0.738. For spillways of small heights and high energy heads, i.e. for $P/H_d < 1.0$, the value of C_{d0} decreases with P/H_d reaching a value of 0.64 at $P/H_d = 0.10$.

The analytical modelling of the spillway flow has been attempted by many investigators. Cassidy[19] has calculated the coefficient of discharge and surface profiles for flow over standard spillway profiles by using the relaxation technique in a complex potential plane. Ikegawa and Washizu[20] have studied the spillway flow through the finite element method (FEM) by making considerable simplification of the basic problem. Diersch et al.[21] have given a generalised FEM solution of gravity flows of ideal fluids and have studied the variation of C_0 with H_0/H_d for a spillway of $P/H_d = 4.29$.

Several experimental data are available on the variation of C_0. It is found that C_0/C_{d0} is essentially a function of H_0/H_d as indicated in Fig. 7.15. It is seen that (C_0/C_{d0}) increases continuously with H_0/H_d. Experiments by Rouse and Reid[17], Cassidy[17], Schirmer and Diersch[21] and the FEM studies of Diersch have revealed that the discharge coefficient ratio C_0/C_d continues to increase with H_0/H_d as shown in Fig. 7.15 up to a certain maximum value of head ratio $(H_0/H_d)_m$. The increased discharge coefficient at $(H_0/H_d) > 1.0$ is due to the occurrence of negative pressures on the crest. At sufficiently high negative pressures, separation of the boundary layer from the crest and consequent decrease in the flow efficiency results. Also, if the minimum negative pressures approach the vapour pressure, cavitation can occur. The maximum head ratio $(H_0/H_d)_m$ thus corresponds to the

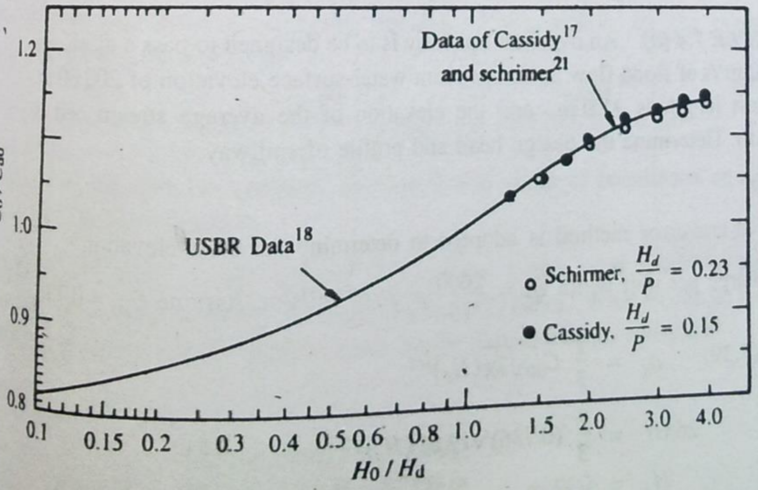

Fig. 7.15 Variation of C_0/C_{d0} with H_0/H_d

onset of separation, and its value is known to depend to a small extent on P/H_d. Experimental studies[17] have shown that there is no possibility of separation and also no pressure fluctuations of any consequence would occur in the overflow spillway operation with $H_0/H_d \le 3.0$, the inception of cavitation is the only problem to be guarded against.

It is seen that the overflow spillway, when working at $1 < H_0/H_d < (H_0/H_d)_m$, has the desirable feature of higher values of the discharge coefficient C_0. This feature can be advantageously exploited in the spillway design. As maximum possible flood flow over a spillway is a rare event, the spillway profile can be designed to correspond to a lower value of head such that at the maximum possible flood, $H_0/H_d > 1.0$. The other structural features can of course be designed to safely accommodate the flood flow. This ensures that the spillway will be functioning at a higher average efficiency over its operating range. When the maximum flood flow occurs, the spillway will perform at a head more than the design head, and consequently, with an enhanced efficiency. This practice of designing is called *underdesigning of the spillway*.

The use of H_0 and H_d, the energy heads, in the discharge equation is not very convenient for discharge estimation. Usually the value of $V_0^2/2g$ is very small relative to the upstream head h_0, where $h_0 = (H_0 - V_0^2/2g)$. For spillways with $h_0/P < 0.50$, the velocity of approach can be assumed to be negligibly small and the relevant head over the crest up to the water surface can be used in place of the energy head, i.e. h_0 and h_d can be used in place of H_0 and H_d respectively.

To approximately estimate the minimum pressure on the spillway p_m, for operations higher than the design head, the experimental data of Cassidy[17] in the form

$$\frac{p_m}{\gamma H_0} = -1.17\left(\frac{H_0}{H_d} - 1\right) \tag{7.41}$$

can be used. This equation is valid in the range of H_d/P from 0.15 to 0.50.

EXAMPLE 7.4 (a) An overflow spillway is to be designed to pass a discharge of 2000 m³/s of flood flow at an upstream water-surface elevation of 200.00 m. The crest length is 75.0 m and the elevation of the average stream bed is 165.00 m. Determine the design head and profile of spillway.

Solution

A trial-and-error method is adopted to determine the crest elevation.

Discharge per unit width $q_d = \dfrac{2000}{75} = 26.67$ m³/s/m. Assume $C_{d0} = 0.736$.

By Eq. (7.39) $$q_d = \frac{2}{3} C_{d0}\sqrt{2g}\,(H_d)^{3/2}$$

$$26.67 = \frac{2}{3}(0.736)\sqrt{19.62}\,(H_d)^{3/2}$$

$$H_d = 5.32 \text{ m}$$

Velocity of approach $V_a = \dfrac{q}{P + h_0} = \dfrac{26.67}{(200.00 - 165.00)}$

$= 0.762$ m/s

$$h_a = \frac{V_a^2}{2g} = 0.0296 \approx 0.03 \text{ m}$$

Elevation of energy line $= 200.03$ m

Crest elevation $= 200.03 - 5.32 = 195.71$ m

$P = 195.71 - 165.00 = 30.71$ m

$$P/H_d = \frac{30.71}{5.32} = 5.77$$

For this value of P/H_d from Fig. 7.14, $C_{d0} = 0.738$.

2nd iteration

$$(H_d)^{3/2} = \frac{26.67}{(2/3)(0.738)\sqrt{19.62}}, \qquad H_d = 5.31 \text{ m}$$

$h_a \approx 0.03$. Elevation of energy line $= 200.03$ m

Crest elevation $200.03 - 5.31 = 194.72$ m

$P = 194.72 - 165.00 = 29.72$ m

$P/H_d = 5.60$. For this P/H_d, from Fig. 7.14, $C_{d0} = 0.738$. Hence no more iterations are required.

Design energy head $H_d = 5.31$ m

and crest elevation $= 194.72$ m

The downstream profile of the crest is calculated by Eq. (7.37), which for the present case is

$$\frac{y}{5.31} = 0.50\left(\frac{x}{5.31}\right)^{1.85}$$

The upstream profile is calculated by Eq. (7.38), which, for the range $0 \le -x \le 1.434$, is given as

$$\frac{y}{5.31} = 0.724\left(\frac{x}{5.31} + 0.270\right)^{1.85} - 0.432\left(\frac{x}{5.31} + 0.270\right)^{0.625} + 0.126$$

The apex of the crest at elevation 194.72 m is the origin of coordinates of the above two profile equations.

EXAMPLE 7.4 (b) In the spillway of Example 7.4(a), what would be the discharge if the water-surface elevation reaches 202.00 m? What would be the minimum pressure on the spillway crest under this discharge condition?

Solution

$$h_0 = 202.00 - 194.72 = 7.28 \text{ m}$$

$$h_0 + P = 202.00 - 165.00 = 37.00 \text{ m}$$

Assuming the velocity of approach head h_a = 0.05 m, the elevation of the energy line = 202.05 m.

$$H_0 = 202.05 - 194.72 = 7.33 \text{ m}$$

$$\frac{H_0}{H_d} = \frac{7.33}{5.31} = 1.38$$

From Fig. 7.15, corresponding to $\frac{H_0}{H_d} = 1.38$, $\frac{C_0}{C_{d0}} = 1.04$.

Since $C_{d0} = 0.738$

$$C_0 = 0.768$$

$$q = \frac{2}{3}\sqrt{19.62}\,(0.768)\,(7.33)^{3/2} = 45.00 \text{ m}^3\text{/s/m}$$

$$V_a = \frac{45.00}{37.00} = 1.216 \text{ m/s}, \quad h_a = \frac{V_a^2}{2g} \approx 0.08 \text{ m}$$

2nd iteration:

Elevation of the energy line = 202.08

$$H_0 = 202.08 - 194.72 = 7.36 \text{ m}$$

$$\frac{H_0}{H_d} = 1.386 \qquad \frac{C_0}{C_{d0}} = 1.04 \text{ from Fig. 7.15,}$$

$$C_0 = 0.768$$

$$q = \frac{2}{3}\sqrt{19.62}\,(0.768)\,(7.36)^{3/2} = 45.28 \text{ m}^3\text{/s/m}$$

V_a = 1.224 m and $h_a \approx$ 0.08 m which is the same as the assumed value at the beginning of this iteration.

Hence

$$H_0 = 7.36 \text{ m}, \; q = 45.28 \text{ m}^3\text{/s/m}$$

$$Q = 45.28 \times 75 = 3396 \text{ m}^3\text{/s}$$

Minimum pressure:

Using Eq. (7.41),

$$\frac{p_m}{\gamma} = -1.17\,(7.36)\,(1.386 - 1)$$

$$= -3.32 \text{ m}$$

The minimum pressure head over the spillway will be 3.32 m below atmospheric.

7.4.2 Contractions on the Spillway

Very often an overflow spillway operates with end contractions. These contractions occur due to the presence of abutments and piers on the spillway to carry a bridge. Equation (7.40) is used to calculate the discharge at any head H_0. The effective length of the spillway L_e is estimated by

$$L_e = L - 2\,(NK_p + K_a)\,H_0 \qquad (7.42)$$

in which L = actual length of the spillway, N = number of piers, K_p = peir contraction coefficient and K_a = abutment contraction coefficient. The values of K_p and K_a depend essentially on the geometry of the contraction-causing element in relation to the flow. For preliminary studies, the following values are usually adopted[18].

Piers:	(i) Square-nosed with rounded corners	$K_p = 0.02$
	(ii) round-nosed	$K_p = 0.01$
	(iii) pointed-nosed	$K_p = 0.00$
Abutments:	(i) Square with sharp corners	$K_a = 0.20$
	(ii) round entry corner	$K_a = 0.10$

7.4.3 Spillway with Crest Gates

When spillways are provided with crest gates, they have to operate as uncontrolled spillway under high flood conditions and with partial gate openings at lower flows. At partial gate openings, the water issues out of the gate opening as an orifice flow and the trajectory is a parabola. If the ogee is shaped by Eq. (7.37), the orifice flow, being of a flatter trajectory curve, will cause negative pressures on the spillway crest. These negative pressures can be minimised if the gate sill is placed downstream of the apex of the crest. In this case the orifice flow will be directed downwards at the initial point itself, causing less difference between the ogee profile and the orifice trajectory.

If the trajectory of the orifice flow with the gate sill located at the apex of the crest is adopted for the spillway profile, the coefficient of discharge at the full-gate opening will be less than that of an equivalent uncontrolled overflow spillway.

The discharge from each bay of a gated ogee spillway is calculated from the following large orifice equation.

$$Q = \frac{2}{3}\sqrt{2g}\, C_g L_b \left(H_0^{3/2} - H_1^{3/2}\right) \tag{7.43}$$

where C_g = coefficient of the gated spillway, L_b = effective length of the bay after allowing for two end contractions, H_0 = energy head above the spillway crest and H_1 = energy head above the bottom edge of the gate (Fig. 7.16). The coefficient of discharge C_g depends upon the geometry of the gate, gate installation, interference of adjacent gates and flow conditions. For radial gates, an approximate value of the coefficient of discharge C_g can be expressed by using the USBR data[18] as

$$C_g = 0.615 + 0.104\,\frac{H_1}{H_0} \quad \text{for} \quad \frac{H_1}{H_0} < 0.83 \tag{7.44}$$

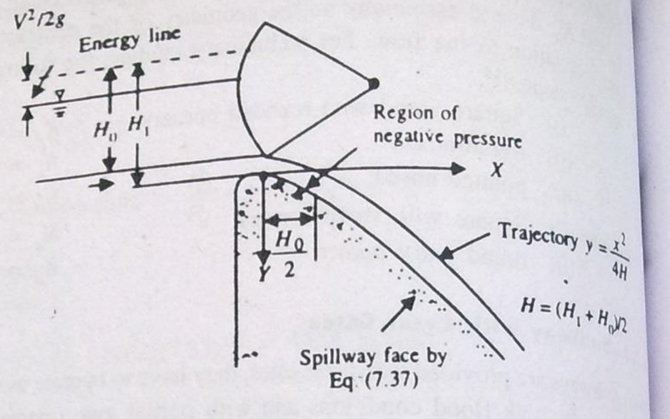

Fig. 7.16 Flow under a crest gate

7.5 BROAD-CRESTED WEIR

Weirs with a finite crest width in the direction of flow are called *broad-crested weirs*. They are also termed as *weirs with finite crest width* and find extensive applications as control structures and flow measuring devices. It is practically impossible to generalise their behaviour because a wide variety of crest and cross-sectional shapes of the weir are used in practice. In this section the salient flow characteristics of only a simple, rectangular, horizontal broad-crested weir presented.

Figure 7.17 is a definition sketch of a free flow over a horizontal broad-crested weir in a rectangular channel. This weir has a sharp upstream corner which causes the flow to separate and then reattach enclosing a separation bubble. If the width B_w of the weir is sufficiently long, the curvature of the stream lines will be small and the hydrostatic pressure distribution will prevail over most of its width. The weir will act like an inlet with subcritical flow upstream of the weir and supercritical flow over it. A critical-depth control section will occur at the upstream end-probably at a location where the bubble thickness is maximum.

Assuming no loss of energy between sections 1 and 2 (Fig. 7.17), and further assuming the depth of flow at section 2 to be critical,

$$H = y_c + \frac{V_c^2}{2g} = \frac{3}{2}\, y_c$$

$$V_c = \sqrt{g y_c} \quad \text{and} \quad y_c = \frac{2}{3}\, H$$

The ideal discharge per unit width of the weir is

$$q_t = V_c y_c = \frac{2}{3}\sqrt{\left(\frac{2}{3}\, g\right)}\; H^{3/2} = 1.705\; H^{3/2} \qquad (7.45)$$

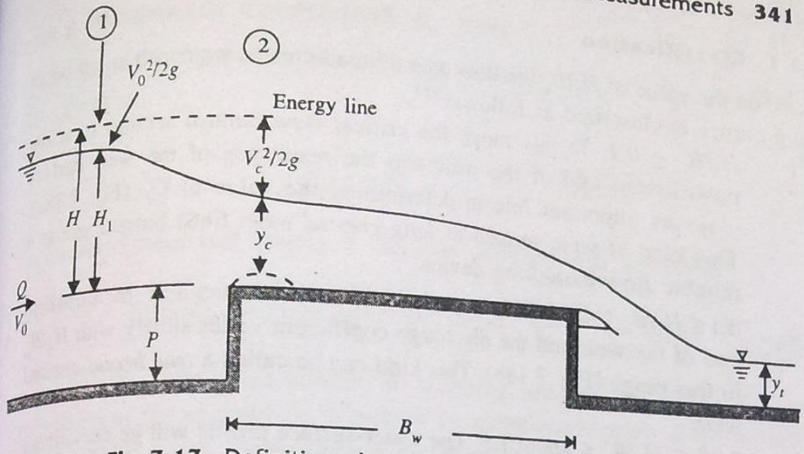

Fig. 7.17 Definition sketch of a broad-crested weir

To account for the energy losses and the depth at section 2 being not strictly equal to the critical depth, the coefficient of discharge C_{d1} is introduced in Eq. (7.45) to get an equation for the actual discharge q as

$$q = C_{d1}\, q_t$$
$$= 1.705\; C_{d1} H^{3/2} \qquad (7.46)$$

and $Q = qL$, where L = length of the weir.

It may be noted that in connection with broad-crested weirs, L = length of the weir measured in a transverse direction to the flow and B_w = width of the weir measured in the longitudinal directon. Thus B_w is measured at right angles to L. In suppressed weirs $L = B$ = width of the channel. This terminology is apt to be confusing and as such warrants a clear understanding of each of these terms.

Since Eq. (7.46) is rather inconvenient to use as it contains the energy head H, an alternate form of the discharge equation commonly in use is

$$Q = \frac{2}{3}\, C_d \sqrt{2g}\; L H_1^{3/2} \qquad (7.47)$$

where H_1 = height of the water-surface elevation above the weir surface measured sufficiently upstream of the weir face and C_d = the coefficient of discharge.

If the upstream end is rounded, the separation bubble will not exist and instead, a boundary layer will grow over the weir with the critical-depth control point shifting towards this downstream end. The flow over most part of its crest will be subcritical. Considerable flow resistance from the upstream face to the critical flow section exists, influencing the value of C_d. The round-nosed broad-crested weir is not dealt with in this section and the details on it are available in Ref. 4.

7.5.1 Classification

Based on the value of H_1/B_w the flow over a broad-crested weir with an upstream sharp corner is classified as follows[22,23].

1. $H_1/B_w \leq 0.1$: In this range the critical flow control section is at the downstream end of the weir and the resistance of the weir surface plays as important role in determining the value of C_d (Fig. 7.18a). This kind of weir, termed as *long-crested weir*, finds limited use as a reliable flow-measuring device.
2. $0.1 \leq H_1/B_w \leq 0.35$: The critical depth control occurs near the upstream end of the weir and the discharge coefficient varies slowly with H_1/B_w in this range (Fig. 7.18b). This kind can be called a *true broad-crested weir.*
3. $0.35 \leq H_1/B_w \leq$ about 1.5: The water-surface profile will be curvilinear all over the weir. The control section will be at the upstream end (Fig. 7.18c). The weirs of this kind can be termed as *narrow-crested* weirs. The upper limit of this range depends upon the value of H_1/P.
4. $H_1/B_w >$ about 1.5: The flow separates at the upstream corner and jumps clear across the weir crest. The flow surface is highly curved (Fig. 7.18d), and the weir can be classified as sharp-crested.

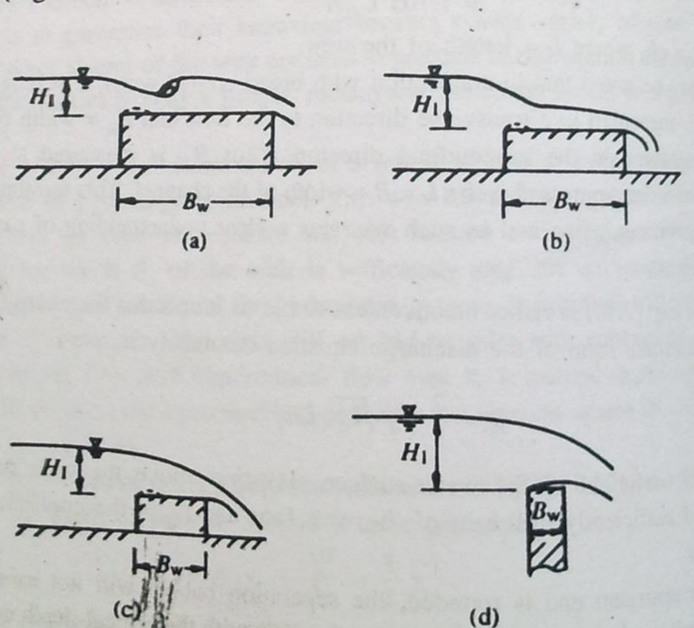

Fig. 7.18 (a) Long-crested weir ($H_1/B_w \leq 0.1$)
(b) Broad-crested weir ($0.1 \leq H/B_w \leq 0.35$)
(c) Narrow-crested weir ($0.35 \leq H_1/B_w \leq 1.5$)
(d) Sharp-crested weir ($H_1/B_w \geq 1.5$)

7.5.2 DISCHARGE COEFFICIENTS, C_d AND C_{d1}

From Eqs (7.47) and (7.46) the discharge coefficients C_d and C_{d1} respectively are given as

$$C_d = \frac{Q}{\frac{2}{3}\sqrt{2g}\,LH_1^{3/2}} \quad \text{and} \quad C_{d1} = \frac{Q}{1.705\,LH^{3/2}} \tag{7.48}$$

A formal dimensional analysis of the flow situation will reveal that

$$C_d (\text{or } C_{d1}) = f\left[\frac{H_1}{L}, \frac{H_1}{B_w}, \frac{H_1}{P}, Re, W, \frac{k_s}{H_1}\right] \tag{7.49}$$

in which Re = Reynolds number, W = Weber number and k_s/H_1 = relative roughness of the weir surface. In most of the situations of practical interest with broad crested weirs, the parameters Re, W, k_s/H_1 and H_1/L have insignificant effect on C_d (or C_{d1}). Hence for practical purposes,

$$C_d (\text{or } C_{d1}) = f\,(H_1/B_w \text{ and } H_1/P) \tag{7.50}$$

Considerable experimental investigations have been conducted to study the variation of C_d (or C_{d1}) as indicated by Eq. (7.50). Lakshmana Rao[1] has given a good bibliography on these studies. Govinda Rao and Muralidhar[22] on the basis of extensive studies of the weir of finite crest in the range $0 \le H_1/B_w \le 2.0$ and $0 \le H_1/P \le 1.0$, have given the following expressions for the variation of C_d:

1. For long weirs, $H_1/B_w \le 0.1$

$$C_d = 0.561\,(H_1/B_w)^{0.022} \tag{7.51}$$

2. For broad-crested weirs, $0.1 \le H_1/B_w \le 0.35$

$$C_d = 0.028\,(H_1/B_w) + 0.521 \tag{7.52}$$

3. For narrow-crested weirs, $0.45 \lesssim H_1/B_w \lesssim$ about 1.5

$$C_d = 0.120\,(H_1/B_w) + 0.492 \tag{7.53}$$

The upper limit of H_1/B_w in Eq (7.53) depends on H_1/P.

Between cases 2 and 3, there exists a small transition range in which Eq. (7.52) progressively changes into Eq. (7.53). In this transition region Eq. (7.52) can be used up to $H_1/B_w \le 0.40$ and Eq. (7.53) for $H_1/B_w > 0.40$. It may be noted that Eq. (7.51) through Eq. (7.53) show C_d as a function of H_1/B_w only and the parameter H_1/P has no effect on C_d in the range of data used in the derivation of these equations. Surya Rao and Shukla[24] have conclusively demonstrated the dependence of C_d on H_1/P. As such Eqs (7.51), (7.52) and (7.53) are limited to the range $0 \le H_1/P \le 1.0$.

Singer[23] has studied the variation of C_{d1} for values of H_1/B_w up to 1.5 and H_1/P up to 1.5. For the range $0.08 \le H_1/B_w \le 0.33$ and $H_1/P < 0.54$, the value of C_{d1} is found to remain constant at a value of 0.848. For higher values of H_1/B_w as well as H_1/P, the coefficient C_{d1} is a function of both these parameters.

7.5.3 Submerged Flow

If the tailwater surface elevation measured above the weir crest $H_2 = (y_1 - P)$ (Fig. 7.19) is appreciable, the flow over the crest may be entirely subcritical. The discharge in such a case will depend upon both H_1 and H_2. The submergence (modular) limit depends upon H_1/B_w and in the broad-crested weir flow range, it is of the order of 65 per cent. At this value, the downstream water surface drowns the critical depth on the crest. For submergences larger than the modular limit, the coefficient of discharge (C_d or C_{d1}) decreases with the submergence ratio H_2/H_1 at a rapid rate. Compared to the sharp-crested weir, the broad-crested weir has very good submergence characteristics.

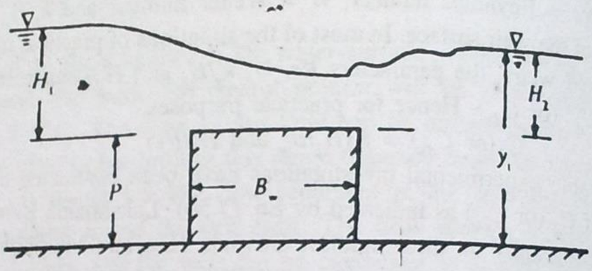

Fig. 7.19 Submerged broad-crested weir flow

EXAMPLE 7.5 A broad-crested weir with an upstream square corner and spanning the full width of a rectangular canal of width 2.0 m is planned. The proposed crest length is 2.50 m and the crest elevation is 1.20 m above the bed. Calculate the water-surface elevation upstream of the weir when the discharge is (a) 2.0 m³/s and (b) 3.50 m³/s.

Solution

(a) $Q = 2.0 \text{ m}^3/\text{s}$

Assume the weir to function in the broad-crested weir mode and hence assume $C_d = 0.525$ as a first guess. From Eq. (7.47)

$$2.0 = \frac{2}{3} \times 0.525 \times \sqrt{19.62} \times 2.0 \times H_1^{3/2}$$

$$H_1^{3/2} = 0.645 \text{ and } H_1 = 0.747 \text{ m}$$

$$\frac{H_1}{B_w} = 0.299$$

By Eq. (7.33), $C_d = 0.028\,(0.299) + 0.521 = 0.529$

Substituting this C_d value in Eq. (7.47)

$$H_1^{3/2} = 0.640,\ H_1 = 0.743 \text{ m and from Eq. (7.52)}$$

$$C_d = 0.529$$

Hence the water-surface elevation above the bed = 1.943 m.

(b) $Q = 3.25 \text{ m}^3/\text{s}$

Since Q is higher than in case (a), it is likely that $H_1/B_w > 0.35$. Hence assuming the weir to function in the narrow-crested weir mode, the calculations are started by assuming $C_d = 0.55$.

Ist iteration: $C_d = 0.55$

$$\text{From Eq. (7.28)}, \quad 3.50 = \frac{2}{3} \times 0.55 \times \sqrt{19.62} \times 2.0 \times H_1^{3/2}$$

$$H_1^{3/2} = 1.077, \; H_1 = 1.05\,\text{m}, \; \frac{H_1}{B_w} = 0.42$$

The weir flow is in the transition region between the broad-crested and narrow-crested weir modes. Hence, by Eq. (7.53),

$$C_d = 0.120 \times (0.42) + 0.492 = 0.534$$

2nd iteration: Using $C_d = 0.534$ in Eq. (7.47)

$$H_1^{3/2} = 1.109, \; H_1 = 1.071\,\text{m}, \; \frac{H_1}{B_w} = 0.429$$

From Eq. (7.53), $C_d = 0.543$

3rd iteration: $H_1^{3/2} = 1.091, \; H_1 = 1.060\,\text{m}. \; \dfrac{H_1}{B_w} = 0.424$

$$C_d = 0.543$$

Hence. $H_1 = 1.060$ and the water-surface elevation above the bed is 2.260 m.

7.6 CRITICAL-DEPTH FLUMES

Critical-depth flumes are flow-measuring devices in which a control section is achieved through the creation of a critical-flow section by a predominant width constriction. In practice, these are like broad-crested weirs but with a major change that these are essentially flow-measuring devices and cannot be used for flow-regulation purposes. A typical critical-depth flume consists of a constricted portion called the *throat* and a diverging section. Sometimes a hump is also provided to assist in the formation of critical flow in the throat (Fig. 7.20).

7.6.1 Standing-wave Flume

The critical-depth flume shown in Fig. 7.20 is known as a *standing-wave flume* or *throated flume*. This flume can be fitted into any shape of the parent channel. The throat is prismatic and can be of any convenient shape. Thus for a rectangular parent channel, it is convenient to have a rectangular throat, and for a circular sewer, a circular throat is preferable. A hydraulic jump forms on the downstream of the throat and holds back the tailwater. If the throat is submerged by the tailwater, subcritical flow prevails all over the flume. It is usual to operate the flume in the free-flow mode only, i.e. with the throat unsubmerged.

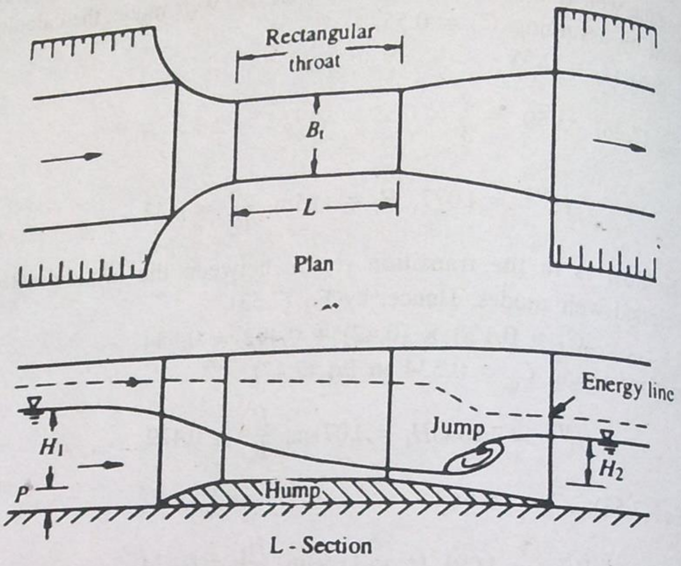

Fig. 7.20 Standing-wave flume

During the operation a critical depth is formed somewhere in the throat and as such its discharge equation is similar to that of a broad-crested weir [Eq. (7.46)]. However, it is usual to relate the discharge to the upstream depth H_1 which can be typically recorded by an automated float equipment. Thus for a rectangular throat section, the discharge is given by

$$Q = C_f \, B_t \, H_1^{3/2} \tag{7.54}$$

where C_f = overall discharge coefficient of the flume = $f(H_1/L)$. For a well-designed flume, C_f is of the order of 1.62. It may be noted that in standing-wave flumes, H_1 is the difference in the water-surface elevation upstream of the inlet and the elevation of the crest at the throat. If the flume is submerged and the subcritical flow prevails all over the flume, Eq. (7.54) is not valid and two depth measurements are needed to estimate the discharge. Constriction flumes operating in the subcritical flow range are called *venturi flumes*.

The modular limit (H_2/H_1) of standing wave flumes is high, being of the order of 0.90. It is usual to take it as 0.75 to incorporate a small safety factor and to avoid the region of transition from the free to submerged-flow mode.

Large varieties of standing-wave flumes with different types of modifications of the basic type described above, resulting in different geometric shapes and corresponding flow characteristics are in use[4,5]. However, the basic favourable features of all these throated flumes can be summarised as: (i) low energy loss, (ii) rugged construction, (iii) easy passage for floating and suspended material load and (iv) high modular limit. These features are responsible for extensive use of throated flumes as flow-measuring devices in water-treatment plants and in mirrigation practice.

EXAMPLE 7.6 (a) A standing-wave flume without a hump is to be provided in a rectangular channel of bottom width = 2.0 m, n = 0.015 and S_0 = 0.0004. A maximum discharge of 2.50 m^3/s is expected to be passed in this flume. If the modular limit of the flume is 0.75, find the width of the throat. (Assume C_f = 1.62.)

Solution

$$\phi = \frac{Qn}{\sqrt{S_0}\,B^{8/3}} = \frac{2.5 \times (0.015)}{\sqrt{0.0004}\ (2.0)^{8/3}} = 0.29529$$

From Table 3A.1, $\frac{y_0}{B}$ (corresponding to m = 0) = 0.656 and normal depth y_0 = 1.312 m. This is the tailwater depth H_2.

For a modular limit of 0.75, $H_1 = \frac{1.312}{0.75} = 1.749$ m

By Eq. (7.54), $B_t = \frac{Q}{C_f\, H_1^{3/2}} = \frac{2.50}{1.62 \times (1.749)^{3/2}}$

$= 0.667$ m

EXAMPLE 7.6 (b) In the Example 7.6(a) compare the heading up of water surface (afflux) due to the flume and also due to a suppressed free flowing sharp-crested weir.

Solution

From Example 7.6(a) heading up (afflux) due to flume

$= H_1 - H_2 = 1.749 - 1.312 = 0.427$ m

Sharp-crested weir

For free-flow operation, the crest of the weir should be at least 0.08 m above the tailwater elevation. Hence $P = 1.312 + 0.080 = 1.392$ m.

Ist trial: Assume C_d = 0.650

By Eq. (7.5) $Q = \frac{2}{3} C_d \sqrt{2g}\, L\, h_1^{3/2}$

h_1 = head over the crest

$$h_1^{3/2} = \frac{2.50}{\frac{2}{3} \times 0.65 \times 2.0 \times \sqrt{19.62}} = 0.651,\ h_1 = 0.751 \text{ m}$$

$\frac{h_1}{P}$ = 0.54 and by Rehbock equation [Eq. (7.7)],

$C_d = 0.611 + 0.08(0.54) = 0.654$

2nd trial: Using C_d = 0.654

$h_1^{3/2} = 0.651 \times \frac{0.650}{0.654} = 0.647,\ h_1 = 0.748$ m

h_1/P = 0.537 and C_d = 0.654

Hence h_1 = 0.748 m

Afflux = 0.748 + 1.392 − 1.312 = 0.828 m

7.6.2 Parshall Flume

The Parshall flume is a type of critical-depth flume popular in the USA. This flume consists of a converging section with a level floor, a throat with a downstream sloping floor and a diverging section with an adverse slope bed (Fig. 7.21). Unlike in the standing-wave flume, the head (H_a) is measured at a specified location in the converging section. The discharge in the flume in the free flow mode is given by

$$Q = K H_a^n \tag{7.55}$$

where K and n are constants for a given flume. The dimensions of various sizes of Parshall flumes are standardised and further details are available in Refs 4, 5, 25 and 26.

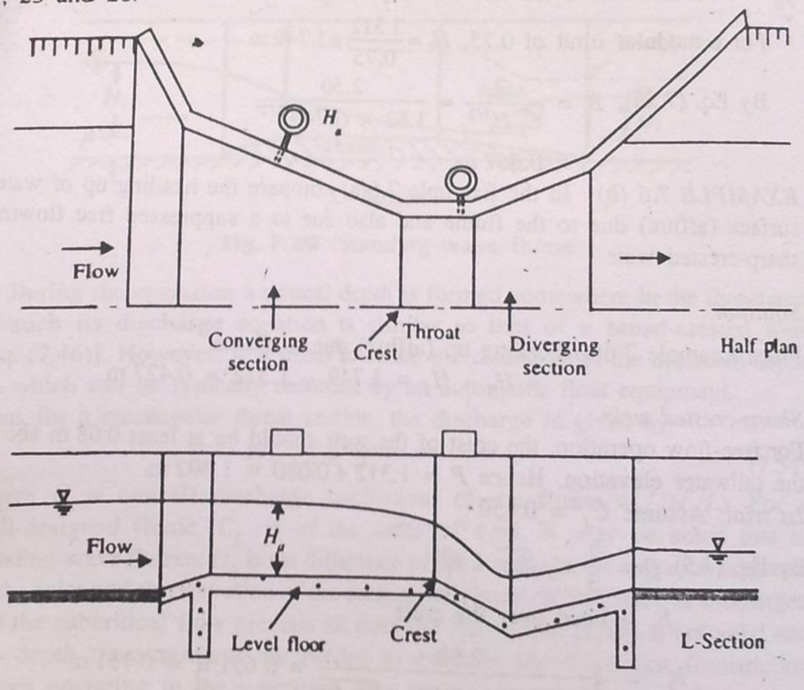

Fig. 7.21 Parshall flume

7.7 END DEPTH IN A FREE OVERFALL

A free overfall is a situation in which there is a sudden drop in the bed causing the flow to separate from the stream bed and move down the step with a free nappe. The situation is analogous to the flow over a sharp-crested weir of zero height. A free overfall causes not only a GVF profile in the subcritical flow, but also offers the possibility of being used as a flow measuring device in all flow regimes.

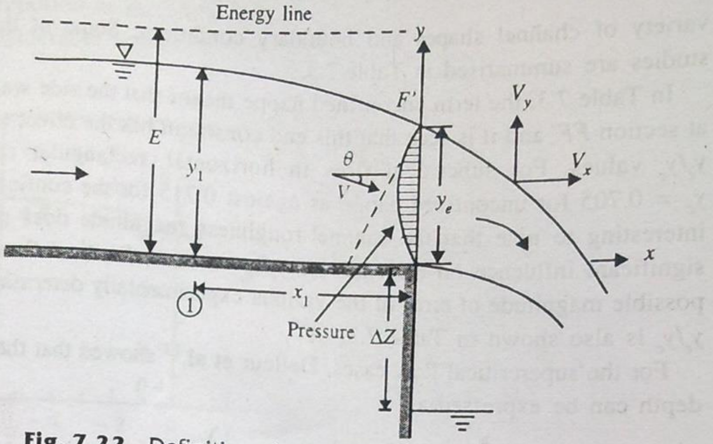

Fig. 7.22 Definition sketch of the end depth

A typical free overfall is schematically illustrated in Fig. 7.22. The flow in the nappe emerging out of the overfall is obviously affected by gravity. With the atmospheric pressure existing above and below the nappe, the water-surface profile is a parabola. Due to the need for continuity of the water-surface profile, the gravity effect extends a short distance on the water-surface profile behind the edge, causing an acceleration of the flow. Also, at the brink, the pressure should necessarily be atmospheric at points *F* and *F'*. This causes the pressure distribution at section *FF'* to depart from the hydrostatic-pressure distribution and assume a pattern as shown in Fig. 7.22. At sections upstream of the brink, the water-surface curvature gradually decreases and at a section such as *1*, at a distance x_1 from *F*, the full hydrostatic pressure is re-established. The result of this effect of the free overfall is to cause a reduction in the depth from section *1* in the down stream direction with the minimum depth y_e occurring at the brink. This depth y_e is known as the *end depth* or the *brink depth*.

In subcritical flow a critical section must occur if the flow has to pass over to supercritical state. The critical depth y_c based on hydrostatic pressure distribution will occur upstream of the brink. In Fig. 7.22 section *1* can be taken as the critical section with $y_1 = y_c$. Then $x_1 = x_c$.

In supercritical flow, y_1 will be equal to the normal depth, $y_1 = y_0$.

7.7.1 Experimental Observations

Rouse[27] was probably the first to recognise the interesting feature of the end depth at a free fall. His experiments on the end depth for subcritical flow in a horizontal rectangular channel with side walls continuing down stream on either side of the free nappe with atmospheric pressure existing on the upper and lower sides of the nappe (confined nappe) indicated that $y_e = 0.715\ y_c$. Since then a large number of experimental studies have been conducted on a variety of channel shapes and boundary conditions. Some of the important studies are summarised in Table 7.3.

In Table 7.3, the term unconfined nappe means that the side walls terminate at section FF' and it is seen that this end constraint has the effect of decreasing y_e/y_c values. For subcritical flow in horizontal, rectangular channels, $y_e/y_c = 0.705$ for unconfined nappe as against 0.715 for the confined case. It is interesting to note that the channel-roughness magnitude does not have any significant influence on the value of y_e/y_c in the subcritical flow range. The possible magnitude of error of the various experimentally determined values of y_e/y_c is also shown in Table 7.3.

For the supercritical flow cases, Delleur et al.[23] showed that the relative end depth can be expressed as

$$\frac{y_e}{y_c} = f\left(\frac{S_0}{S_c}, \text{ channel shape}\right) \tag{7.56}$$

For a given channel, the variation of y_e/y_c can be expressed as a unique function of S_0/S_c. The results of some experimental observations on rectangular channels are indicated in Fig. 7.23. Similar variations of y_e/y_c with S_0/S_c for triangular,

Table 7.3 Experimental Results on End Depth in Subcritical Flow in Horizontal Channels

End conditions: C = confined nappe, U = unconfined nappe

SL. No.	Shape	Investigator(s)	End conditions	$\frac{y_e}{y_c}$	Variation (approx.) per cent	Remarks
1	Rectangular	Rouse[27]	C	0.715		
		Krainjenhoff et al.[5]	C	0.715	± 2.0	No effect of roughness
			U	0.705	± 2.0	-do-
		Rajaratnam[31] and Muralidhar[28,31]	C	0.715	± 3.5	
			U	0.705		
2	Circular	Rajaratnam and Muralidhar[29]	U	0.725	± 3.5	No effect of roughness
3	Triangular	Rajaratnam and Muralidhar[28]	U	0.795	± 2.0	Fully developed approach flow
4	Parabolic	Rajaratnam and Muralidhar[28]	U	0.772	± 5.0	-do-
5	Trapezoidal	Diskin[32]	U	$f\left[\frac{my_c}{B}\right]$		
		Rajaratnam and Muralidhar[30]	U	$f\left[\frac{my_c}{B}\right]$	± 5.0	

parabolic, circular and trapezoidal channels recorded in various experimental studies are reported in the literature[1]. In experimental studies on large values of S_0/S_c, considerable scatter of data, of the order ±10 per cent, is observed.

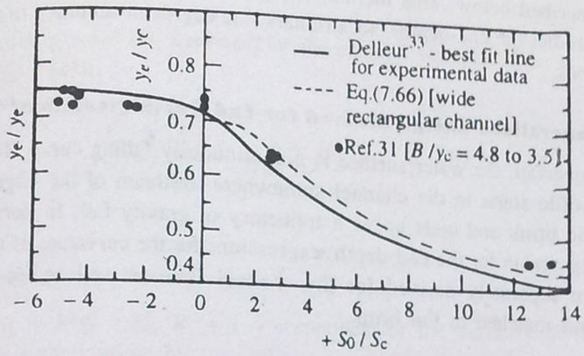

Fig. 7.23 End-depth ratio in rectangular channels

Experimental studies[34] have shown that in subcritical flow $\frac{x_e}{y_c}$ is of the order of 3.0 to 6.0 and is a function of the Froude number of the flow. Further, if the brink flow is not to be affected by the tailwater level, the drop Δz (Fig. 7.22) should be greater than 0.6 y_c (Ref. 5).

7.7.2 Analytical Studies

For the prediction of end depth, several analytical attempts have been made by earlier workers. Most of them are based on the application of the momentum equation with various assumptions, especially regarding the velocity and pressure distributions at the brink section. In a typical momentum approach[28,29,32] the pressure force at the brink section is expressed as $P_e = \gamma A_e \bar{y}_e K_1$, when K_1 = a pressure-correction factor and $\bar{y}_e$ = the depth of the centre of gravity below the free surface at the brink section. The success of the momentum equation to predict y_e depends upon the proper choice of K_1 (the variation of K_1 with the geometry of the problem has to be determined experimentally).

The numerical solution of a two-dimensional ideal fluid-flow at a free overfall has been attempted by some investigators through various finite difference schemes. An excellent review of these studies on potential flow in a free overfall and a theory describing such a flow is presented by Strelkoff et al.[35] While it is possible to solve the end-depth problem in a wide rectangular channel through advanced numerical techniques, such as the finite-element method, the solution of the problem in channels of different shapes have to be tackled by alternative methods.

An elegant method which differs from the above two approaches has been reported by Anderson[34]. Based on Anderson's work, a generalised energy method for the prediction of end-depth in channels of any shape is given by Subramanya[36] and is described below. This method is simple, does not need any coefficient and can predict the end-depths to a remarkable degree of accuracy in a variety of situations.

7.7.3 Generalised Energy Method for End Depth Prediction[36]

In a free overfall, the water surface is a continuously falling curve. The water surface profile starts in the channel somewhere upstream of the edge, passes through the brink and ends up as a trajectory of gravity fall. In deriving the general expression for the end-depth, expressions for the curvature of the water surface are separately derived for the channel flow as well as for the free overfall and matched at the brink.

(a) *Curvature of the channel flow*

Consider a channel of any shape having a free over fall (Fig. 7.22). The water surface curvature is assumed to be relatively small and is assumed to vary linearly from a finite value at the surface to zero value at the channel bottom. The effective piezometric head is then expressed by the Boussinesq equation [Eq. (1.33)]. The water surface curvature is convex upwards and the specific energy E at any section is given by Eq. (1.41) as

$$E = h_{ep} + \alpha \frac{V^2}{2g}$$

By using Eq. (1.33) for h_{ep}

$$E = y + \alpha \frac{V^2}{2g} + \frac{1}{3}\frac{V^2 y}{g}\left(\frac{d^2y}{dx^2}\right) \tag{7.57}$$

i.e.

$$E = y + \alpha \frac{Q^2}{2g A^2} + \frac{1}{3}\frac{Q^2}{g A^2}\, y\left(\frac{d^2y}{dx^2}\right) \tag{7.58}$$

Assume the specific energy E to be constant in the neighbourhood of the brink and further assume $\alpha = 1.0$ for simplicity. The conditions at the brink section (denoted by the suffix e) is expressed, by non-dimensionalising Eq. (7.58) with respect to the critical depth y_c, as

$$\frac{E_e}{y_c} = \frac{y_e}{y_c} + \frac{Q^2}{2g A_e^2 y_c} + \frac{1}{3}\frac{Q^2}{g A_e^2 y_c}\frac{y_e}{y_c}\frac{d^2(y/y_c)}{d(x/y_c)^2}\Bigg|_{y = y_e} \tag{7.59}$$

Denoting the critical conditions by the suffix c,

$$y_e/y_c = \eta;\quad \frac{A_c^3}{A_e^2 T_c y_c} = f(\eta) \quad \text{and} \quad E_e/y_c = \varepsilon$$

Remembering that $Q^2/g = A_c^3/T_c$ Eq. (7.59) can be simplified as

$$\varepsilon = \eta + \frac{1}{2} f(\eta) + \frac{1}{3} \eta f(\eta) \left. \frac{d^2(y/y_c)}{d(x/y_c)^2} \right|_{y = y_e} \tag{7.60}$$

The expression for the curvature of the channel water surface at the brink is from Eq. (7.60),

$$\left. \frac{d^2(y/y_c)}{d(x/y_c)^2} \right|_{y = y_e} = \frac{3}{\eta f(\eta)} \left[\varepsilon - \eta - \frac{1}{2} f(\eta)\right] \tag{7.61}$$

(b) Overflow trajectory

Referring to Fig. 7.22, $V_x = x$ – component of the velocity in the overflow trajectory and is given by

$$V_x = V_e \cos\theta \tag{7.62}$$

where V_e = mean velocity at the brink inclined at an angle θ to the horizontal. For a gravity fall

$$\frac{dV_x}{dt} = 0 \text{ and } \frac{dV_y}{dt} = -g$$

where $V_y = y$ – component of the velocity in the trajectory.

Since $\dfrac{dy}{dx} = \dfrac{V_y}{V_x}$

$$\frac{d^2y}{dx^2} = -g/V_x^2 = -\frac{gA_e^2}{(V_e A_e)^2 \cos^2\theta}$$

$$= -\frac{gA_e^2}{Q^2 \cos^2\theta} \tag{7.63}$$

Noting that $\dfrac{Q^2}{g} = \dfrac{A_c^3}{T_c}$, Eq. (7.63) can be written as

$$\frac{d^2y}{dx^2} = -\frac{T_c A_e^2}{A_c^3 \cos^2\theta} = -\frac{1}{y_c f(\eta) \cos^2\theta}$$

Thus,

$$\left. \frac{d^2(y/y_c)}{d(x/y_c)^2} \right|_{y = y_e} = -\frac{1}{f(\eta) \cos^2\theta} \tag{7.64}$$

(c) General equation for end depth ratio

For a continuous water surface slope at $(x = 0, y = y_e)$ Eq. (7.61) and Eq. (7.64) must be identical and as such

$$-\frac{1}{f(\eta)\cos^2\theta} = \frac{3}{\eta f(\eta)}\left[\varepsilon - \eta - \frac{1}{2} f(\eta)\right]$$

Simplifying,

$$6\,\varepsilon\,\cos^2\theta - 2\,\eta\,(3\cos^2\theta - 1) - 3\,f(\eta)\,\cos^2\theta = 0 \qquad (7.65)$$

In the usual cases when θ is small, $\cos\theta \approx 1.0$, $\cos^2\theta \approx 1.0$ and Eq. (7.65) simplifies to

$$6\varepsilon - 4\eta - 3\,f(\eta) = 0 \qquad (7.66)$$

This equation is the general equation relating the end-depth ratio η with the non-dimensionalised specific energy at the brink and is based on the assumption of constancy of the specific energy in the neighbourhood of the brink. To illustrate the use of Eq. (7.66), the prediction of end-depth in exponential channels is presented in the following section.

7.7.4 End Depth in Exponential Channels

An exponential channel is defined as the one in which the area A is related to the depth y as $A = Ky^a$, where K and a are constants. It is easily seen that a = 1.0, 1.5 and 2.0 represents rectangular, parabolic and triangular channels respectively.

For exponential channels, $T = \dfrac{dA}{dy} = K\,a\,y^{a-1}$ and $\dfrac{A}{T} = \dfrac{y}{a}$ (7.67)

$$f(\eta) = \frac{A_c^3}{A_e^2}\,\frac{1}{T_c y_c} = \frac{1}{a}\,(y_c/y_e)^{2a} = \frac{1}{a\eta^{2a}} \qquad (7.68)$$

Eq. (7.66) now becomes

$$6\varepsilon - 4\eta - \frac{3}{a}\,\frac{1}{\eta^{2a}} = 0 \qquad (7.69)$$

The solution of Eq. (7.69) is now obtained for subcritical and supercritical channel flows separately.

(I) Subcritical flow

If the flow upstream of the brink is subcritical, the critical depth must occur before the end-depth. Assuming constant specific energy E between the critical section and end section

$$\varepsilon = \frac{E_e}{y_c} = \frac{E_c}{y_c}$$

Since $E_c = y_c + \frac{Q^2}{2g A_c^2} = y_c + \frac{A_c}{2T_c}$

$$\varepsilon = 1 + \frac{1}{2}\left(\frac{A_c}{T_c}\frac{1}{y_c}\right)$$

By substituting Eq. (7.67), for an exponential channel

$$\varepsilon = 1 + \frac{1}{2a} \tag{7.70}$$

Thus for a given exponential channel shape (i.e. a = constant), ε is constant for subcritical flow.

Eq. (7.69) now becomes

$$6\left(1 + \frac{1}{2a}\right) - 4\eta - \frac{3}{a}\frac{1}{\eta^{2a}} = 0$$

and can be solved for a given value of a. It is seen that for a given value of a, the end-depth ratio η is a constant in subcritical flow and is independent of the flow parameters like Froude number.

(II) Supercritical flow

If the flow upstream of the brink is supercritical, the normal depth y_0 is less than y_c and the critical depth does not exist in the profile between y_c and y_e. Considering a section between y_0 and y_e (Fig. 7.24)

$$\varepsilon = \frac{E_e}{y_c} = \frac{E_0}{y_c} = \frac{y_0}{y_c} + \frac{Q^2}{2g A_0^2 y_c}$$

Putting $\frac{y_0}{y_c} = \delta$ and, noting that $\frac{Q^2 T_0}{g A_0^3} = F_0^2$

$$\varepsilon = \delta + \frac{F_0^2}{2}\cdot\frac{A_0}{T_0 y_0}$$

$$= \delta + \frac{F_0^2}{2} f(\delta) \tag{7.71}$$

where $f(\delta) = \frac{A_0}{T_0 y_c}$ (7.72a)

In an exponential channel $f(\delta) = \delta / a$

$$\text{and} \quad F_0^2 = \frac{A_c^3 T_0}{A_0^3 T_c} = \left(\frac{y_c}{y_0}\right)^{2a+1} = \left(\frac{1}{\delta}\right)^{2a+1} \tag{7.72b}$$

$$\text{or} \quad \frac{y_0}{y_c} = \delta = \left[\frac{1}{F_0^{2/(2a+1)}}\right] \tag{7.72c}$$

Thus for an exponential channel having supercritical flow upstream of the brink, by substituting Eqs (7.72a, b, and c) in Eq. (7.71) it is seen that ε is a function of the upstream Froude number F_0 given by

$$\varepsilon = \frac{1}{F_0^{2/(2a+1)}}\left(1 + \frac{F_0^2}{2a}\right)$$

$$\eta = fn\,(a,\, F_0) \tag{7.74}$$

End depth ratios in exponential channels

Using Eq. (7.69) along with appropriate expression for ε, [*viz.* Eq. (7.70) in subcritical flow and Eq. (7.73) in supercritical flow], the value of the end-depth ratio η can be evaluated for a given flow situation. Table 7.4 gives the values of η for subcritical flows in rectangular, parabolic and triangular channels evaluated by Eq. (7.69) along with the corresponding results obtained experimentally.

Table 7.4 Comparison of End Depth Ratios of η Obtained by Eq. (7.69)

Channel shape	*a*	$\eta = \frac{y_e}{y_c}$ *by Eq. (7.69)*	*Mean experimental value (Table 7.3)*	*Per cent under estimation*
Rectangle	1.0	0.694	0.715 ± 3.5%	2.9
Parabola	1.5	0.734	0.772 ± 5.0%	4.9
Triangle	2.0	0.762	0.795 ± 2.5%	4.2

Generally, the predictions are less by about 5% of the mean experimental values, probably due to the neglect of frictional effects. Considering the nature of scatter of experimental results, the prediction of η by Eq. (7.69) can be taken as satisfactory and adequate.

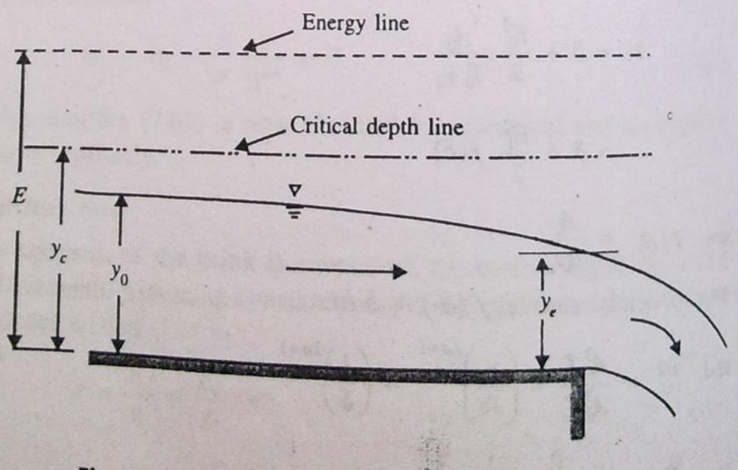

Fig. 7.24 Free overfall in supercritical flow

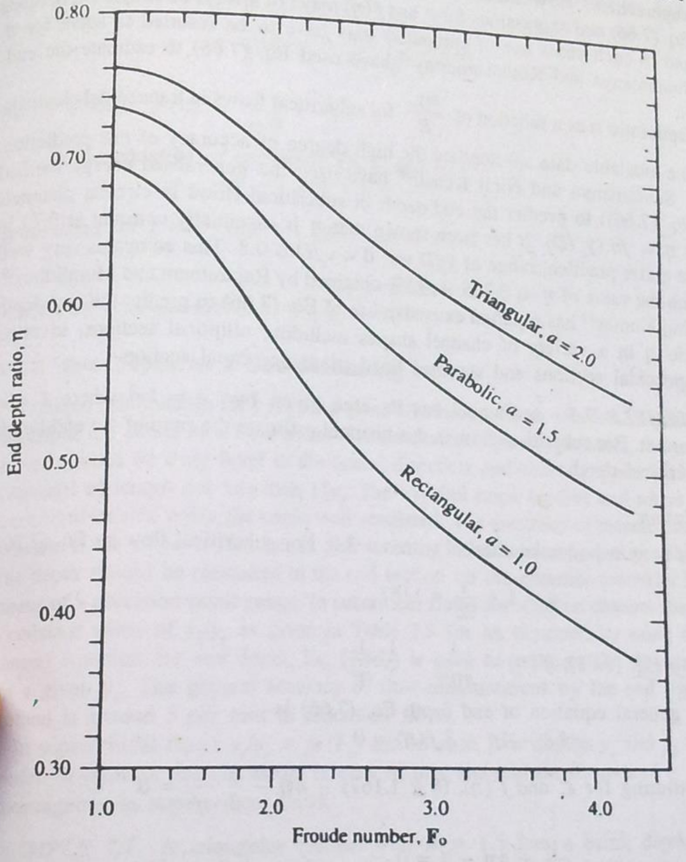

Fig. 7.25 Variation of the end depth ratio in supercritical flows

Figure 7.25 shows the variation of the end-depth ratio η with F_0 for supercritical flows, in rectangular, parabolic and triangular channels, obtained by solving Eq. (7.69). Detailed experimental data are not available to verify these predictions completely. However, available data on triangular channels[27] have shown the prediction to be satisfactory. Satisfactory comparison of available data in rectangular channels is shown in Fig. 7.23.

7.7.5 End Depth in Other Channel Shapes

The generalised energy method described in the earlier section is a simple and versatile technique to predict the end-depth ratio η in both subcritical and supercritical flow modes in prismatic channels of any shape. However, Eq. (7.66) and expressions for ε and $f(\eta)$ may not always be simple expressions and in such cases use of computers may have to be resorted to solve for η. Subramanya and Keshavamurthy[37] have used Eq. (7.66) to estimate the end-depth ratio η as a function of $\frac{my_e}{B}$ for subcritical flows in trapezoidal channels. The available data substantiate the high degree of accuracy of this prediction.

Subramanya and Niraj Kumar[38] have used the generalised energy method (Eq. (7.66)) to predict the end-depth in subcritical flows in circular channels as $\eta = fn\ (y_c/D)$. It has been shown that η is essentially constant at 0.73 in the entire practical range of y_c/D viz. $0 < y_c/D \le 0.8$. This compares very well with the value of $\eta = 0.725 \pm 3.5\%$ obtained by Rajaratnam and Muralidhar[29]. Niraj Kumar[39] has reported extensive use of Eq. (7.66) to predict the end-depth ratio η in a variety of channel shapes including elliptical sections, inverted trapezoidal sections and standard lined triangular canal section.

EXAMPLE 7.5 A channel has its area given by $A = ky^3$ where k = a constant. For subcritical flow in this channel estimate the ratio of the end-depth to critical depth.

Solution

This is an exponential channel with $a = 3.0$. For subcritical flow by Eq. (7.70)

$$\varepsilon = 1 + \frac{1}{2a} = 1.167$$

By Eq. (7.68), $f(\eta) = \dfrac{1}{a\eta^{2a}} = \dfrac{1}{3}\dfrac{1}{\eta^6}$

The general equation of end depth Eq. (7.66) is

$$6\varepsilon - 4\eta - 3\,f(\eta) = 0$$

Substituting for ε and $f(\eta)$, $(6 \times 1.167) - 4\eta - \dfrac{3}{3}\dfrac{1}{\eta^6} = 0$

i.e. $$\frac{1}{\eta^6} + 4\eta - 7 = 0$$

Solving by trial and error $\eta = y_e/y_c = 0.80$.

EXAMPLE 7.6 A rectangular channel carries a supercritical flow with a Froude number of 2.0. Find the end-depth ratio at a free overfall in this channel.

Solution

In supercritical flow, for an exponential channel, $\varepsilon = fn(a, F_0)$.

Here $a = 1.0$

By Eq. (7.53) $$\varepsilon = \frac{1}{F_0^{2/(2a+1)}}\left(1 + \frac{F_0^2}{2a}\right)$$

$$= \frac{1}{2^{2/(2+1)}}\left(1+\frac{2^2}{(2\times 1)}\right) = 1.89$$

By Eq. (7.68), $f(\eta) = \dfrac{1}{a\eta^{2a}} = \dfrac{1}{\eta^2}$

The general equation of end-depth, Eq. (7.66) is

$$6\varepsilon - 4\eta - 3\, f(\eta) = 0$$

Substituting for ε and $f(\eta)$, $6 \times 1.89 - 4\eta - \dfrac{3}{\eta^2} =$

i.e. $$4\,\eta^3 - 11.34 + 3 = 0$$

Solving by trial-and-error, $\eta = y_e/y_c = 0.577$.

7.7.6 End Depth as a Flow-Measuring Device

The unique relationship for y_e/y_c for a given channel at a free overfall has given end depth the status of a flow meter. For flow-measurement purposes, the end section should be truly level in the lateral direction and must be preceded by a channel of length not less than $15y_c$. The overfall must be free and where it is confined by side walls, the nappe well ventilated. The accuracy of measurement is better if the slope is flat, i.e. as near to being a horizontal bed as possible. The depth should be measured at the end section on the channel centreline by means of a precision point gauge. In subcritical flows for a given channel shape a constant value of y_e/y_c as given in Table 7.3 (or as obtained by using the general equation for end depth, Eq. (7.66)) is used to estimate the discharge for a given y_e. The general accuracy of flow-measurement by the end depth method is around 3 per cent in subcritical flows.

In supercritical flows $y_e/y_c = fn\,(F_0)$ and as such two depths y_e and y_0 are needed to estimate the discharge. In view of this, the end-depth method is not advantageous in supercritical flows.

EXAMPLE 7.7 A triangular channel with $m = 1.5$ has a brink depth of 0.6 m at a free overfall. Estimate the discharge in the channel if the flow is known to be subcritical.

Solution

Taking the experimentally observed result (Table 7.3) of $y_e/y_c = 0.795$ for subcritical flow in triangular channels

$$y_c = \frac{0.6}{0.795} = 0.755$$

For a triangular channel from Eq. (2.14)

$$y_c = (2Q^2/g\,m^2)^{1/5}$$

i.e. $$Q = (gm^2 y_c^5/2)^{1/2} = \left[\frac{9.81(1.5)^2\,(0.755)^5}{2}\right]^{1/2}$$

$$= 1.645 \text{ m}^3\text{/s}$$

PROBLEMS

Problem Distribution

	Topic	Problems
1.	Rectangular weir	7.1 – 7.7; 7.19
2.	Weirs of various shapes	7.4
3.	Triangular weir	7.5
4.	Sutro weir	7.8, 7.10
5.	Quadratic weir	7.9, 7.11
6.	Ogee spillway	7.12 – 7.16
7.	Broad crested weir	7.17 – 7.20
8.	Critical depth flume	7.21, 7.22
9.	End depth	7.23 – 7.28
10.	Sluice gate	7.29 – 7.34

7.1 A rectangular sharp-crested suppressed weir is 2.0 m long and 0.6 m high. Estimate the discharge when the depth of flow upstream of the weir is 0.90 m. If the same discharge was to pass over an alternative contracted weir of 1.5 m length and 0.60 m height at the same location, what would be the change in the water-surface elevation?

7.2 A sharp-crested suppressed weir is 1.5 m long. Calculate the height of the weir required to pass a flow of 0.75 m^3/s while maintaining an upstream depth of flow of 1.50 m.

7.3 A rectangular sharp-crested suppressed weir is 3.0 m long and 1.2 m high. During a high flow in the channel, the weir was submerged.with the depths of flow of 1.93 m and 1.35 m at the upstream and downstream of the weir respectively. Estimate the discharge.

7.4 Develop expressions as given in Table 7.2 for the discharge over triangular, circular, parabolic and trapezoidal sharp-crested weirs.

7.5 A right angled triangular notch discharges under submerged condition. Estimate the discharge if the heights of water surface measured above the vertex of the notch on the upstream and downstream of the notch plate are 0.30 m and 0.15 m respectively (Assume $C_d = 0.58$).

7.6 A 15 m high sharp-crested weir plate is installed at the end of a 2.0 m wide rectangular channel. The channel side walls are 1.0 m high. What maximum discharge can be passed in the channel if the prescribed minimum free board is 20 cm ?

7.7 A sharp-crested weir of height 0.80 m and length 2.0 m was fitted with a point gauge for recording the head of flow. After some use, the point gauge was found to have a zero crror; it was reading heads 2 cm too small. Determine the percentage error in the estimated discharges corresponding to an observed head of 50 cm.

7.8 Design a Sutro weir for use in a 0.30 m wide rectangular channel to have linear discharge relationship in the discharge range from 0.25 m^3/s to 0.60 m^3/s. The base of the weir will have to span the full width of the channel. Assume $C_d = 0.62$.

7.9 Design a quadratic weir spanning the full width of a 0.50 m rectangular channel at the base and capable of passing minimum and maximum discharges of 0.10 m^3/s and 0.40 m^3/s respectively under the desired proportionality relationship. (Assume C_d = 0.61.)

7.10 A Sutro weir with a rectangular base is installed in a rectangular channel of width 60 cm. The base weir spans the full width of the channel, has its crest coinciding with the channel bed; and has a height of 12 cm. (i) Estimate the discharge through the channel when the depth of flow in the channel immediately behind the weir is 25 cm. (ii) What discharge in the channel is indicated when the depth of flow is 33 cm? (iii) What depth of flow in the channel can be expected for a discharge of 0.20 m^3/s? [Take C_d = 0.61].

7.11 A quadratic weir with rectangular base of 45 cm width and 9 cm height has a depth of flow of 15 cm in the channel. Estimate (i) the discharge through the weir and (ii) the depth of flow in the channel corresponding to a discharge of 25 litres/s. [Take C_d = 0.61].

7.12 Find the elevation of the water surface and energy line corresponding to a design discharge of 500 m^3/s passing over a spillway of crest length 42 m and crest height 20 m above the river bed. What would be the energy head and minimum pressure head when the discharge is 700 m^3/s?

7.13 A spillway with a crest height of 25.0 m above the stream bed is designed for an energy head of 3.5 m. If a minimum pressure head of 5.0 m below atmospheric is allowed, what is the allowable discharge intensity over the spillway?

7.14 A spillway has a crest height of 30.0 m above the bed and a design energy head of 3.0 m. The crest length of the spillway is 50 m. As a part of remodelling of the dam, a three-span bridge is proposed over the spillway. The piers will be 1.5 m thick and are round-nosed and the abutment corners will be rounded. What will be the change in the water-surface elevation for the design-flood discharge?

7.15 An overflow spillway with its crest 15 m above the river bed level has radial gates fitted on the crest. During a certain flow, the water surface upstream of the dam was observed to be 2.5 m above the crest and the gate opening was 1.0 m. Estimate the discharge from a bay of 15.0 m length. (Neglect end contractions.)

7.16 An ogee spillway with a vertical face is designed to pass a flood flow of 250 m^3/s. The distance between the abutments of the spillway is 45.0 m. A three-span bridge is provided over the spillway. The bridge piers are 1.20 m wide and are round nosed. If the crest of the spillway is 10.0 m above the river bed level, find the elevaiions of the water surface and energy line. Using this discharge as the design discharge, calculate the spillway crest profile.

7.17 A rectangular channel 2.5 m wide has a broad-crested weir of height 1.0 m and a crest width of 1.5 m built at a section. The weir spans the full canal width. If the water-surface elevation above the crest is 0.5 m, estimate the discharge passing over the weir. If the same discharge passes over another similar weir, but with a crest width of 2.5 m, what would be the water-surface elevation upstream of this second weir?

7.18 A broad-crested weir of height 2.0 m and width 3.0 m spans the full width of a rectangular channel of width 4.0 m. The channel is used as an outlet for excess water from a tank of surface area 0.5 hectares at the weir crest level. If the water level in the tank at a certain time is 0.90 m above the weir crest, what is the discharge over the weir? Estimate the time taken to lower the water-surface elevation by 60 cm. (Assume that there is no inflow into the tank and the surface area of the tank is constant in this range.)

7.19 A rectangular channel 2.0 m wide carrying a discharge of 2.5 m^3/s is to be fitted with a weir at its downstream end to provide a means of flow measurement as well as to cause heading-up of the water surface. Two choices, viz. (i) a sharp-crested weir plate of 0.80 m high and (ii) a broad-crested weir block of 0.80 m height and 1.0 m width, both spanning the full width of the channel, are considered. Which of these weirs causes a higher heading-up and to what extent?

7.20 Show that for a triangular broad crested weir flowing free the discharge equation can be expressed as

$$Q = \frac{16}{25} C_{d1} \tan\theta \sqrt{(2/5)g}\; H^{5/2}$$

where H = energy head measured from the vertex of the weir, θ = semi-apex angle and C_{d1} = coefficient of discharge.

7.21 A standing wave flume is used to measure the discharge in a 10.0 m wide rectangular channel. A 5 m wide throat section has a hump of 0.5 m height. What is the discharge indicated when the upstream depth of flow in the channel at the flume entrance is 2.10 m? Assume an overall coefficient of discharge of 1.620 for the flume.

7.22 A rectangular throated flume is to be used to measure the discharge in a 9.0 m wide channel. It is known that the submergence limit for the flume is 0.80 and the overall discharge coefficient is 1.535. A throat width of 5.0 m is preferred. What should be the height of the hump if the flume is to be capable of measuring a discharge of 20.0 m^3/s as a free flow with the tailwater depth at 2.30 m?

7.23 Obtain the end-depth ratio $\eta = \dfrac{y_e}{y_c}$ for a triangular channel having (a) subcritical flow and (b) supercritical flow with a Froude number of 2.5.

7.24 Show that for a channel whose area $A = k\, y^{2.5}$ the end-depth ratio η for subcritical flow mode is 0.783. Also, determine the variation of η with Froude number F_0 for supercritical flow in the channel.

7.25 A parabolic channel with a profile $x^2 = 4ay$, where y axis is in the vertical direction, terminates in a free fall. Show that the end-depth ratio $\eta = y_e/y_c$ for supercritical flow is given by

$$2\,\eta^4 - 4\,\eta^3 + 1 = 0$$

Determine the relevant root of this equation and compare it with the experimentally obtained value of η.

7.26 Find the end depth at a free overfall in a rectangular channel when the upstream flow is at a Froude number of 3.0 with a normal depth of 0.70 m.

7.27 Estimate the discharges corresponding to the following end-depth values in various channels. The channels are horizontal and the flow is subcritical in all cases.

(i) Rectangular channel, $B = 2.0$ m, $y_e = 0.6$ m
(ii) Triangular channels, $m = 1.0$, $y_e = 0.5$ m
(iii) Circular channel, $D = 0.90$ m, $y_e = 0.3$ m

[*Hint*: Use the value of y_e/y_c given in Table 7.3.]

7.28 Write a general mometum equation to the flow at the end-depth region in an exponential channel ($A = ky^a$). Assuming the channel to be horizontal without any friction and the pressure force at the brink to be $P_e = \gamma \bar{y}_e A_e K_1$, show that

$$K_1 = \frac{1}{\varepsilon_r^{a+1}} - \left(\frac{a+1}{a}\right)\frac{(1-\varepsilon_r^a)}{\varepsilon_r^{2a}+1}$$

where $\varepsilon_r = y_e/y_c$.

7.29 A rectangular channel 2.0 m wide has its depth backed-up to a height of 1.2 m by a sharp-edged sluice gate. If the gate opening is 0.30 m and the downstream flow is free, estimate the discharge through the gate and the force on the gate.

7.30 A rectangular channel 2.0 m wide has to pass a flow of 2.4 m^3/s through a sluice gate opening of 0.4 m. If the water depth upstream of the gate is 2.0 m, find the depth of water immediately below the gate.

7.31 A rectangular channel carries a discharge of 2.5 m^3/s/m. Find the opening of a sluice gate required to pass this flow with an upstream depth of 4.0 m. The sluice gate can be assumed to be operating under free-flow conditions.

7.32 Apply the momentum equation to the submerged sluice gate flow (Fig. 7.29) by making suitable assumptions and estimate the depth H_2 immediately below the sluice gate in terms of y_t, a, C_c and H_1.

7.33 Obtain an expression for the force on the sluice gate in submerged flow for the situation in Fig. 7.29.

7.34 Show that the modular limit of the free flow in a sluice gate (Fig. 7.29) is given by

$$\frac{y_t}{a} = \frac{C_c}{2}\left[-1+\sqrt{1+8F_{1c}^2}\right]$$

where $F_{1c}^2 = \left(\frac{C_d^2}{C_c^2}\right)\left(\frac{H_1}{a} - C_c\right)$ and y_t = tailwater depth.

OBJECTIVE QUESTIONS

7.1 The head over a 3.0 cm sharp-crested sill is 96 cm. The discharge coefficient C_d for use in the weir formula is
(a) 0.738 (b) 0.848 (c) 0.611 (d) 1.11

7.2 A suppressed sharp-crested weir is 0.50 m high and carries a flow with a head of 2.0 m over the weir crest. The discharge coefficient C_d for the weir is
(a) 1.06 (b) 0.931 (c) 0.738 (d) 0.611

7.3 The discharge Q in a triangular weir varies as
(a) $H^{0.5}$ (b) $H^{1.5}$ (c) $H^{2.0}$ (d) $H^{2.5}$

7.4 In a triangular notch there is a +2% error in the observation of the head. The error in the computed discharge is
(a) +2% (b) +5% (c) −5% (d) +2.5%

7.5 A nominal 90° triangular notch was found to have 2% error in the vertex angle. While discharging under a constant head, the error in the estimated discharge is
(a) π % (b) π /4% (c) π /2% (d) 2%

7.6 In submerged flow over sharp-crested rectangular weirs the Villemonte equation relates Q_s/Q_1 as equal to

(a) $\left[1-\left(\frac{H_2}{H_1}\right)\right]^{-0.385}$ (b) $\left[1-\left(\frac{H_2}{H_1}\right)^{0.385}\right]^{1.5}$

(c) $\left[1-\left(\frac{H_2}{H_1}\right)^{1.5}\right]^{0.385}$ (d) $\left[1+\left(\frac{H_2}{H_1}\right)^{0.385}\right]^{1.5}$

7.7 In a triangular notch the tailwater head is 50% of the upstream head, both measured above the vertex of the notch. If the free flow discharge under the same upstream head is 0.5 m^3/s, the submerged flow, in m^3/s, is
(a) 0.464 (b) 0.411 (c) 0.500 (d) 0.532

7.8 A parabolic sharp-crested weir has a profile given by $x^2 = ky$. The discharge in the weir is given by $Q = K\,H^n$ where n is
(a) 0.5 (b) 1.5 (c) 2.0 (d) 2.5

7.9 A separate arrangement for aeration of the nappe is necessary in a
(a) contracted rectangular weir
(b) suppressed rectangular weir
(c) submerged contracted rectangular weir
(d) triangular weir

7.10 In a linear proportional weir with a rectangular base of height a, the discharges are linearly proportional to the head h_d measured above a datum. The minimum head at which the linear head-discharge relation is observed is h_d =
(a) a (b) $a/2$ (c) $a/3$ (d) $2a/3$

7.11 In a quadratic weir the measured head above the datum was found to have an error of 2%. This would mean that the discharges estimated from the weir discharge formula will have an error of
(a) 0.5% (b) 1% (c) 2% (d) 4%

7.12 Designing of the spillway profile to conform to the shape of the nappe of a sharp crested weir makes
(a) the pressures on the spillway crest always positive
(b) the pressures to be positive for $H_0 \geq H_d$
(c) the pressures on the spillway always zero
(d) the pressure on the crest zero for $H_0 = H_d$ only

7.13 If the head H_0 over an overflow spillway is less than the design head H_d'
(a) the pressure on the spillway crest will be negative
(b) the cavitation phenomenon can occur
(c) the separation of the streamlines from the surface can occur
(d) the coefficient of discharge C_0 will be less than the design coefficient of discharge C_{d0}

7.14 The coefficient of discharge C_0 at any head H_0 of a spillway is a function of
(a) $\left(\frac{H_0}{P}\right)$ only
(b) $\left(\frac{H_0}{H_d}\right)$ only
(c) $\left(\frac{H_0}{P}, \frac{H_0}{H_d}\right)$ only
(d) $\frac{P}{H_d}$ only

7.15 A vertical face ogee spillway will have a crest profile downstream of the apex given by $(y/H_d) =$
(a) $0.5\,(x/H_d)^{1.50}$
(b) $0.5\,(x/H_d)^{1.85}$
(c) $1.85\,(x/H_d)^{0.517}$
(d) $2.0\,(x/H_d)^{2.0}$

7.16 A broad-crested weir with $H_1/B_w = 0.5$ and $H_1/p = 1.0$ and a sharp-crested weir with $H_1/p = 1.0$, both span the full width of a canal. If the coefficient of discharge C_d of the weir ($= C_{dw}$), and C_d of the broad-crested weir ($= C_{db}$) are compared, it will be found that
(a) $C_{dw} > C_{db}$
(b) $C_{db} > C_{dw}$
(c) $C_{dw} = C_{db}$
(d) $C_{dw} = C_{db}$ for small H_1 only.

7.17 A finite crest width weir with $H_1/B_w = 0.20$ is classified as a
(a) long-crested weir
(b) broad crested weir
(c) narrow-crested weir
(d) sharp-crested weir

7.18 The modular limit of a sharp-crested weir (M_s), broad-crested weir (M_b) and standing wave flume (M_f) are compared under equivalent conditions. It will be found that
(a) $M_s > M_b > M_f$
(b) $M_s < M_b < M_f$
(c) $M_s > M_b < M_f$
(d) $M_s < M_b > M_f$

7.19 The overall coefficient of discharge of a standing wave flume $C_f = Q/(B_t H_1^{3/2})$ is of the order of
(a) 0.61
(b) 0.95
(c) 3.30
(d) 1.62

7.20 The discharge equation of a Parshall flume is expressed as $Q =$
(a) $K\sqrt{H_a}$
(b) $K\,H_a$
(c) KH_a
(d) $K\,(H_1^{3/2} - H_a^{3/2})$

7.21 The end depth ratio y_e/y_c in a channel carrying subcritical flow is a function of
(a) shape of the channel only
(b) Shape and Manning's coefficient

(c) Normal depth only
(d) Shape and Froude number

7.22 A 2 m wide horizontal rectangular channel carries a discharge 3.0 m^3/s. The flow is subcritical. At a free overfall in this channel the end depth in metres is

(a) 0.438 (b) 0.612 (c) 0.715 (d) 1.488

7.23 A 2.5 m wide rectangular channel is known to be having subcritical flow. If the depth at a free overfall is 0.5 m, the discharge in this channel in, m^3/s, is

(a) 2.56 (b) 4.40 (c) 1.83 (d) 3.50

7.24 Two horizontal channels *A* and *B* of identical widths and depths have roughness such that $(K_s)_A = 2(K_s)_B$. If the discharges observed by the end-depth method in these two channels are denoted as Q_A and Q_B respectively, then it would be found that

(a) $Q_A > Q_B$ (b) $Q_A = \frac{1}{2} Q_B$

(c) $Q_A = Q_B$ (c) $Q_A < Q_B$

7.25 The effective piezometric head h_{ep} at the brink of a free overfall could be represented as

(a) $h_{ep} < y_e$ (b) $h_{ep} > y_e$ (c) $h_{ep} = y_c$ (d) $h_{ep} = y_e$

7.26 If a rectangular channel carrying a discharge of 1.85 $m^3/s/m$ width shows a brink depth of 0.35 m at a free overal, then

(a) the discharge measured is wrong
(b) the end depth is wrongly measured
(c) the flow is subcritical regime
(d) the flow is in the supercritical regime

7.27 In submerged flow through a sluice gate the coefficient of discharge C_{ds} =

(a) $f\left(\frac{a}{H_1}, \frac{y_t}{a}\right)$ (b) C_{SH} (c) C_{df} (d) C_d

7.28 The coefficient of discharge C_d in free sluice gate is related to C_c as

(a) $C_c = \frac{C_c}{\sqrt{1+(C_c a/H_1)^2}}$ (b) $C_d = \frac{C_c a}{H_1\sqrt{1-(C_c a/H_1)^2}}$

(c) $C_d = \frac{C_c}{\sqrt{1-(C_c a/H_1)^2}}$ (d) $C_d = \frac{C_c}{\sqrt{1-\left(\frac{a}{H_1}\right)C_c}}$

7.29 The discharge coefficient C_{SH} in submerged sluicegate flow is

(a) $f(a/H_1)$ (b) $f(y_t/a)$
(c) $f(a/H_1, y_t/a)$ (d) $= C_d$

7.30 Sluice gates used in field applications have

(a) a bevel on the upstream face
(b) a bevel on the downstream face
(c) bevels on both upstream and downstream faces
(d) no bevel.